No 727481 RESERVE

D3.4 v1.0

Network Impedance Characterisation for Active Distribution Networks

The research leading to these results has received funding from the European Union's Horizon 2020 Research and Innovation Programme, under Grant Agreement no 727481.

Project Name	RESERVE
Contractual Delivery Date:	30.09.2018
Actual Delivery Date:	29.09.2018
Contributors:	Alireza Nouri (UCD), Alireza Soroudi (UCD), Andrew Keane (UCD), Sriram Karthik Gurumurthy (RWTH), Markus Mirz(RWTH), Antonello Monti (RWTH)
Workpackage:	WP-3 – Voltage Control
Security:	*PU*
Nature:	R
Version:	1.0
Total number of pages:	49

Abstract:

In this deliverable, first the active voltage management algorithm previously proposed in this project is extended to include a methodology for adaptive voltage control which is able to update the parameters of the proposed AVM algorithm according to the system configuration. From the dynamic voltage control point of view a methodology is developed for Network Impedance Characterisation (NIC) for distribution networks enabled with inverter-based RES.

Keyword list:

Voltage Control, Active Voltage Management, Voltage Stability, Active Distribution Systems, RES, Optimisation, Reactive Power.

Executive Summary

This deliverable presents developed methodologies of two voltage control scenarios. These methodologies have been developed within **Task 3.4**. RWTH have developed an approach for **Network Impedance Characterisation** for active distribution networks and dynamic voltage stability analysis based on the results of this characterisation, while UCD put forward an **Adaptive Active Voltage Management (AVM)** algorithm based on the results of the impedance identification technique presented in this deliverable. Before the practical application, both algorithms are tested by conducting the simulations on the sample distribution systems to validate their effectiveness.

Measurement of real-time grid impedance is required for calculation of dynamic stability margins and virtual output impedance control in the proposed Dynamic Voltage Stability Monitoring (DVSM) scenario. In **chapter 2**, an online non-invasive Wideband System Identification (WSI) tool is developed by RWTH for estimation of the grid impedance. The proposed controller is developed in Labview real-time NI FPGA; however, this algorithm can be generalized as a software component and it can be augmented with the existing inverter controller hardware. This non-invasive feature i.e. null requirements for power level hardware is an added advantage of the proposed technique. Small signal perturbations are injected in the control signal or control references and the simultaneously recorded voltage and current samples are used to calculate and estimate the grid impedance. This deliverable also analyses the complexity and challenges of WSI tool. *Hardware-in-the-loop (HiL)* simulations are performed to validate the proposed method and to understand the requirements for new grid codes/ modification of grid codes.

In **chapter 3**, a resilient active voltage management is proposed. One of the main factors that affect the Volt-var curves in a three-phase unbalanced distribution system is the system configuration, i.e., the network configuration and availability of the system controllable devices. It is quite probable that in operation of a distribution, the system configuration is changed due to the electrical faults, scheduled maintenance, forced outages of the system components and also operation strategies. These may drastically change the critical parameters in the VVCs assigned to each inverter-based DER. Otherwise, the AVM technique may not be effective in different operating conditions and contingencies. In this chapter, the effects of the network configuration and also the availability of the system controllable devices on the proposed AVM algorithm are analysed. The impedance identification technique is used as an option to develop a resilient Volt-var optimisation scheme. The simulation studies given in this chapter show that by adaptively updating the VVCs according to the system configuration, the values of the objective functions will be improved.

The following points summarises this deliverable:

- A real-time grid method for calculation of dynamic stability (SV_A) margins is proposed
- The proposed methodology is an online non-invasive tool and does not endanger the safe operation of distribution network
- The algorithm can be augmented with the existing inverter controller hardware
- This deliverable also analyses the complexity and challenges of the proposed tool
- Several simulations are performed to validate the proposed method and to understand the requirements for new grid codes/ modification of grid codes.
- A resilient active voltage management (SV_B) is proposed for static stability assessment.
- The impact of the network configuration and availability of the system controllable devices on AVM is investigated.
- The simulation studies on resilient AVM show that the values of the objective functions will be improved.

Authors

Partner	Name	e-mail
UCD		
	Alireza Nouri	alireza.nouri@ucd.ie
	Alireza Soroudi	alireza.soroudi@ucd.ie
	Andrew Keane	andrew.keane@ucd.ie
RWTH		
	Sriram Karthik Gurumurthy	Sgurumurthy@eonerc.rwth-aachen.de
	Markus Mirz	Mmirz@eonerc.rwth-aachen.de
	Antonello Monti	Amonti@eonerc.rwth-aachen.de

Table of Contents

1. Introduction

This deliverable is the output of Task **3.4** in work package 3. This task extends the works of **T3.2** and **T3.3,** which were reported in **D3.2** and **D3.3,** to include a methodology for adaptive static voltage control framework. This framework updates the parameters of the active voltage management algorithm according to the system configuration from the static voltage control point of view. **Network Impedance Characterisation technique** is used for updating the control parameters in distribution networks enabled with different controllable devices and dynamic voltage stability analysis based on the results of this characterisation.

From the static voltage control point of view, one of the main factors that affect the Volt-var curves in a three-phase unbalanced distribution system is the network configuration and the availability of the system controllable devices. Comparing to **D3.3**, in this task a proper set of VVCs is first extracted in offline centralised simulations, then assigned to the system controllable devices. For each controllable device, each VVC is associated with a certain system configuration. In online decentralised application, the connection status of the system controllable devices is first approximated based on the impedance identifying technique. The proper set of VVCs are then used to find the reactive power support of the system controllable device. This complementary technique for adaptive voltage control is being developed in RESERVE project that seeks to maintain steady-state operation of voltages in the low voltage distribution systems characterized by high penetration of RES.

From the dynamic stability point of view, after developing an online non-invasive Wideband System Identification (WSI), in order to estimate the grid impedance which works based on injecting small signal perturbations in the control signal and reordering the voltage and current samples, the complexities and challenges of the proposed WSI tool is discussed.

1.1 Task 3.4

This deliverable summarises the activities of **Task 3.4** within the wider context of WP3. The main aim of **WP3** is to bring about a new understanding for the changing landscape that proliferation of the renewable energy sources will have on distribution networks. In this view, **WP3** redefines and introduces the concepts and theories surrounding static voltage control and dynamic voltage stability.

In this task, first the methodology to identify the system impedance at PCC of the controllable RESs is extended to include the active grid case and presence of other sources during the task with correspondent risk of interaction during the identification process. The identified impedance at each PCC is then used to evaluate the static and dynamic voltage stability while other controllable are available. A methodology is also developed for adaptive active voltage management based on the results of impedance identifying technique. In **T3.5** the robustness of this technique will be improved based on the results provided in **D3.5**.

1.2 Objectives of the Work Report in this Deliverable

- An approach for network impedance characterisation and identification, in particular in the case of active distribution networks should be developed.
- Regarding the online network impedance identification, a main extension with respect to literature should be performed: inclusion of the active grid case
- Presence of other sources with correspondent risk of interaction during the task of impedance identification should be taken into account.
- A method should be developed to update the parameters of the voltage control algorithms based on the results of the impedance identification technique.
- Valid simulations of the adaptive voltage control and stability techniques should be conducted.
- Future deliverables and further work should be outlined.

1.3 Outline of the Deliverable

The deliverable details the research efforts completed in the second year of the RESERVE project in developing the voltage control and stability concepts, especially considering the impedance identification results in the active distribution systems in active voltage management algorithm and also stability analysis. The accomplishments within this task exceed that written in the description of work in the grant agreement, as adaptive active voltage management is also addressed in the AVM algorithm. The technical background and simulation test cases are presented in this deliverable. The proposed methodologies are also validated on sample distribution networks.

1.4 How to Read this Document

This deliverable covers the realisation of the adaptive voltage control and stability techniques based on the results of the impedance identification in an active distribution system enabled with different controllable devices with possible chance of conflict between their operations. This document can be read in isolation to other deliverables, yet it follows an introductory deliverable (**D3.1**) that reports on the basic requirements of the active voltage management from the static and dynamic point of views. In **D3.3** and **D3.5** a framework able to use the local information from the different sources to identify the state of health from the static and dynamic voltage control point of views, respectively. **Figure 1-1** shows the placement of deliverable **D3.4** in the wider context of **WP3** as well as interlinked work packages of the RESERVE project. The methodology which is developed here is an extension to the AVM algorithm presented in **D3.3** and will be completed in **D3.5** by proposing a robust supervised but yet decentralised AVM algorithm.

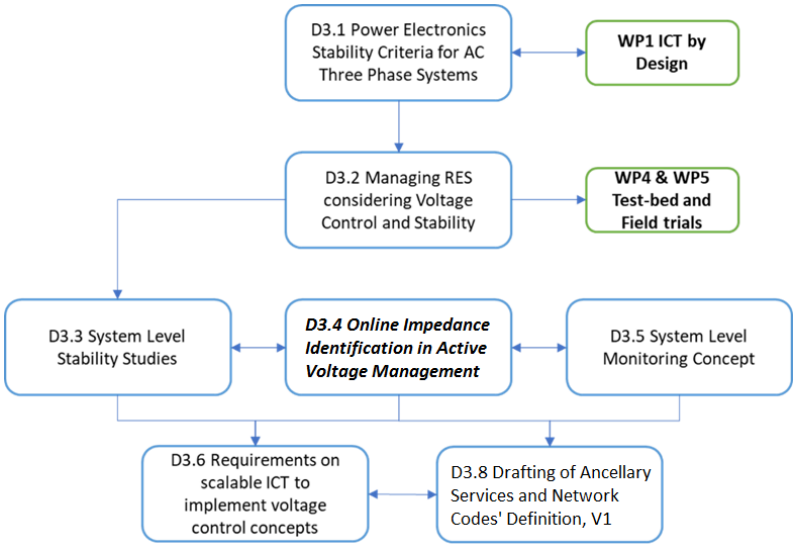

Figure 1-1 Relations between Deliverables in WP3 and other work packages

1.5 Approach Used to Undertake the Work

The following steps were applied to develop the results reported in this deliverable.

- The basic foundation of the new approaches to voltage stability and control are expanded upon from **D3.2 and D3.3** to a simulation environment in **D3.4**.
- Mathematical modelling guarantees the effectiveness of the proposed algorithm for the Dynamic Voltage Stability control and the adaptive AVM algorithm.
- A step-by-step methodology is developed to outline the replicability of the proposed approaches in this deliverable to any desirable unbalanced (or balanced) distribution feeder enabled with different sorts of controllable devices.
- Various case studies are conducted to show the effectiveness of the proposed algorithms for the adaptive active voltage management and also dynamic voltage

stability analysis based on the results of the impedance identification technique presented in this deliverable.

- Conclusions and the future works are presented to summarise the findings of these studies and determine the relation of this deliverable to the future deliverable in this project.

2. The Wideband System Identification technique

2.1 Review of impedance identification techniques

The requirement of measuring the grid impedance is important in order to evaluate the stability of the power electronic interface. Feasibility of offline impedance identification techniques in real power grids are low owing to the ever-changing nature of grid impedance with time. Online methods to measure impedances can monitor system stability in real time and synthesize corrective actions if needed [1].

An important characteristic for the measurement device is the ability to complete the measurement process in a short time. Methods based on sine sweeps are not suitable for online impedance measurements. Another important characteristic for impedance measurement device is that's the process needs to be non-invasive i.e. no requirement of additional power level hardware for the impedance measurement. Certain techniques reported in literature are invasive methods wherein additional power amplifiers and switching passive loads are used [2]–[4]. Such techniques are difficult to implement, and they are very expensive compared to non-invasive methods. Recently, a power electronic based invasive method for grid impedance cancellation [5] and this method is expensive and difficult to implement.

Wideband system identification (WSI) techniques are gaining importance since they use signals which excite the system at all frequencies, thus allowing measurement for a wide range of frequencies in a short time [1], [6]–[11]. These methods fall under the category of non-invasive methods. WSI based impedance identification for power electronics was first introduced in DC applications [1][12]. Further modifications have extended the use of the technique for AC systems. WSI based non-invasive methods for impedance identification of power electronic converters form an interesting conjunction with Power Electronic based LVAC distribution grids [1].

White noise signals or signals that have characteristics of white noise for an interested range of frequencies are injected in the control signal or the reference signal in the control system of the converter [7], [8], [12]. A dedicated platform within the controller records the voltage and current measurements simultaneously and measures the non-parametric impedance. Linear impedance identification techniques are applied to get the parametric impedance model. One of the most widely used band-limited white noise signal is the Psuedo Random Binary Sequence (PRBS) noise which can be easily generated using shift-register concept. The above mentioned techniques inject perturbations when the system is in a steady state and are referred to as steady state techniques [1], [6]–[11]. Transient techniques inject current pulse at impedance measuring point, and the impedance is extracted from its transient response [2], [13], [14]. Steady state methods are preferred since they only perturb the system in a small signal sense whereas transient methods perturb the grid aggressively.

The inverter power stage and its control system is shown in **Figure 2-1**. The above mentioned PRBS noise signal can either by injected in the current reference or in the controller output or combination of both. As shown in **Figure 2-1**, the controller consists of a *d* and *q*-axis where the PRBS noise signals can be superimposed. Sequential measurement of *dq* impedances is adopted in this deliverable similar to [1], [8], [11]. What is Sequential measurement? Firstly, the PRBS is injected along the *d*-axis of the controller and the impedances associated with the d-axis are measured. After the measurement of d-axis impedances are completed, the PRBS is injected in the *q*-axis of the controller and the impedances associated with the q-axis are measured. Due to the time varying nature of impedance, it is advisable to adapt two methods which can measure *dq* impedance simultaneously. Recently, an *dq* impedance estimation method based on orthogonal PRBS generation was reported in [15]. Both *d*- and *q*-axis can be simultaneously perturbed without cross-correlation which enables simultaneous measurement of both *dq* axis impedances.

This chapter reports the WSI tool developed at RWTH lab. WSI technique for three phase systems based on *dq* reference frame is explained and then the components of the proposed non-invasive WSI tool are explained. Experimental validation obtained from *Hardware-in-the-loop (HiL)* shows the accuracy of the proposed technique. Implications on distribution network codes from the proposed technique is also discussed.

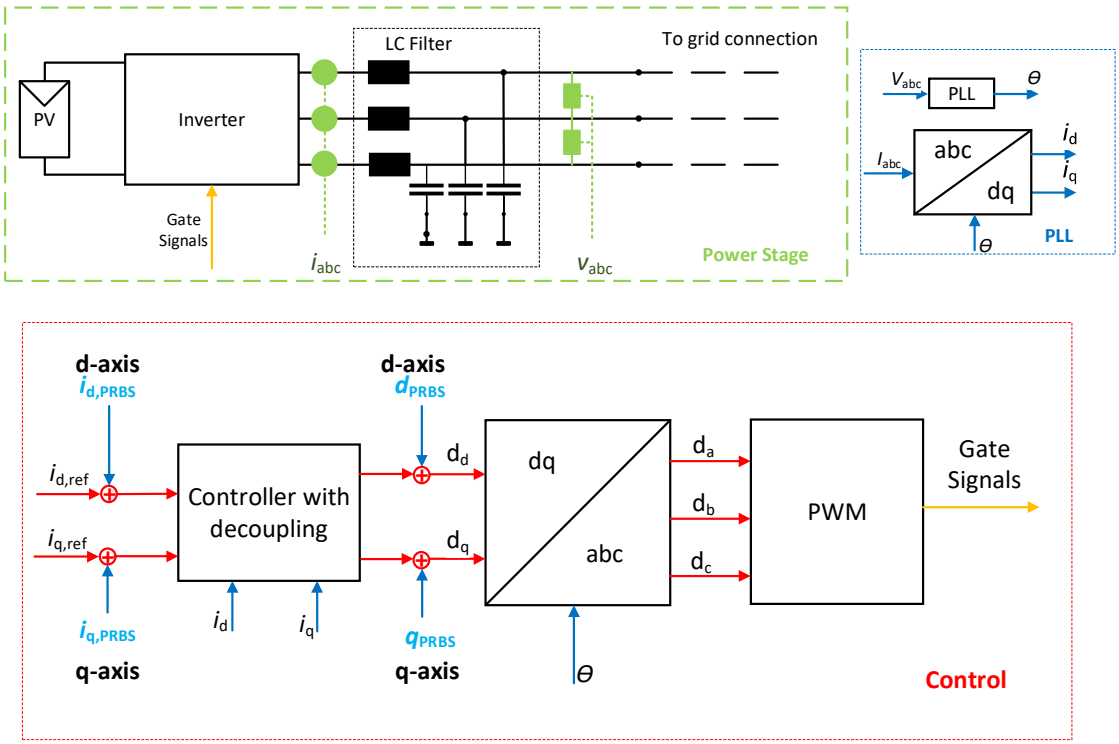

Figure 2-1 PRBS Injection in dq frame

2.2 Impedance identification in *dq* frame of reference

A *dq* impedance matrix takes the form given in (**2.1**). A generic structure of a *dq* impedance based WSI tool is shown in **Figure 2-2**.

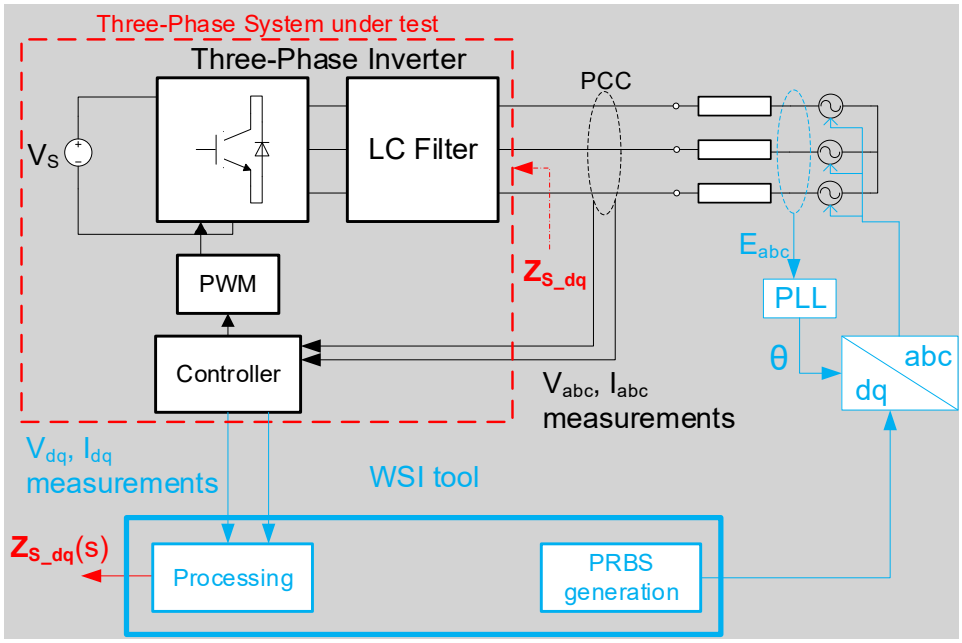

Figure 2-2 WSI technique for estimating DQ Impedances [1]

The measurement of all 4 elements of the matrix in (**2.1**) is done in a sequential manner. The WSI tool injects perturbations in the *d*-axis of the controller through PRBS generation and simultaneously, the three-phase output current and voltages are measured then converted into *dq* domain through the *dq* transformation and stored in a FIFO buffer. The *d*-axis perturbation allows the measurement of Z_{dd} and Z_{dq}. Following which *q*-axis perturbations are injected to

measure Z_{qd} and Z_{qq} impedances. Further post processing allows the computation and estimation of impedance and it is covered in the next section.

$$\boldsymbol{Z} = \begin{bmatrix} Z_{dd} & Z_{dq} \\ Z_{qd} & Z_{qq} \end{bmatrix} \quad (\mathbf{2.1})$$

A slight disadvantage of the above method is the sequential measurements of the impedance matrix components. Due to the time varying nature of impedance, there may be a slight mismatch. To overcome this disadvantage, orthogonal PRBS noise injections are currently being developed and the upcoming versions of WSI tool will have the orthogonal PRBS noise generation, a slight modification to the existing PRBS generation algorithm. With this change, we can inject PRBS noise in both *d* and *q* axis simultaneously which allows simultaneous measurement and estimation of all 4 impedances.

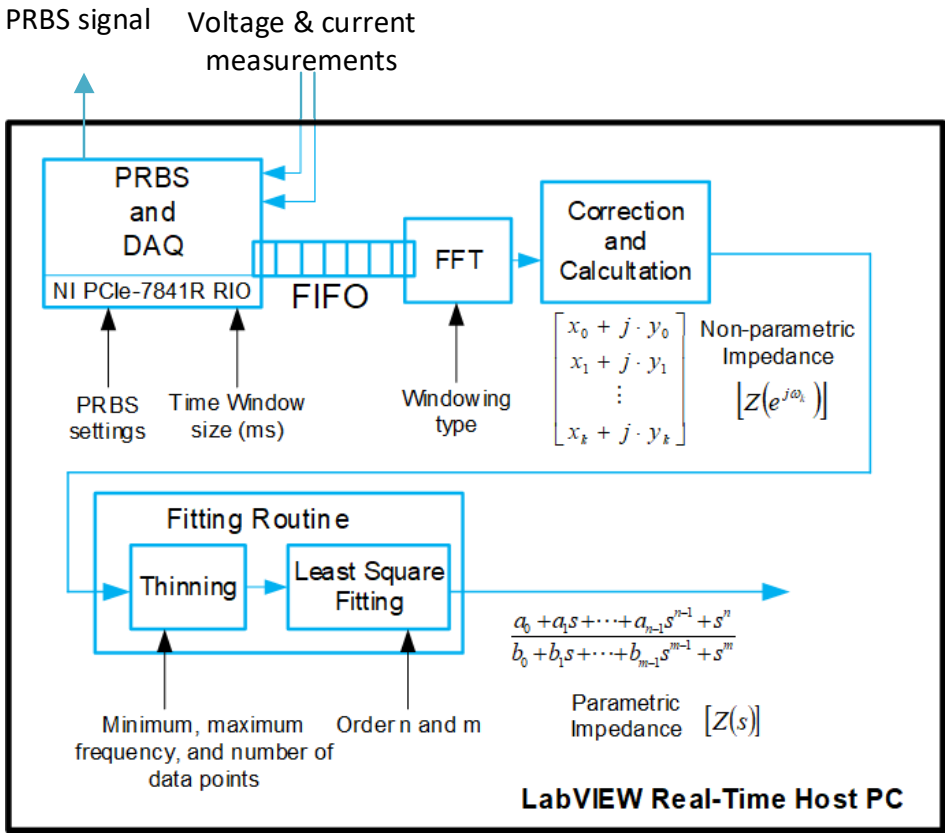

Figure 2-3 WSI tool in SV_A

2.3 The WSI technique and its components

The Various components of the WSI tool and their role in the process of impedance measurement and estimation is covered. The developed Labview based WSI tool is shown in Figure 2-2.

2.3.1 PRBS Generation

A 15-bit linear feedback shift-register (LFSR) is used to generate the PRBS. The XOR-ed value of bit 14 and bit 15 are fed back to the beginning of the register, as depicted in **Figure 2-4**. The output from the last bit of the LFSR is used to scale up as per requirement and level shift to achieve a white-noise approximation with zero mean [9], [12]. The PRBS signal is then properly scaled and added to the duty cycles and the control reference signals of the inverter. Adhering to grid codes, it is recommended to produce a perturbation of 5% of the steady-state operating point.

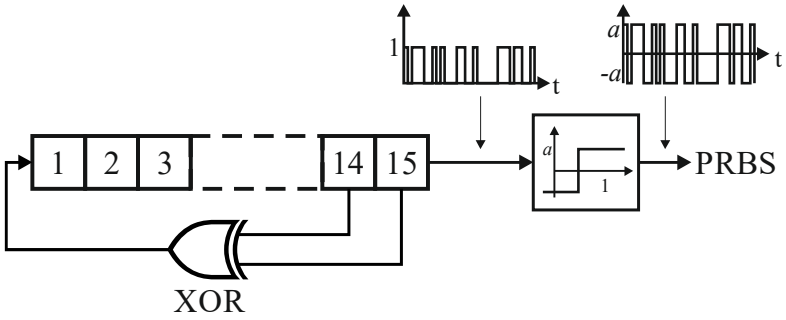

Figure 2-4 LFSR based PRBS generator [1]

2.3.2 Data Acquisition (DAQ)

The PRBS injection and voltage/current data acquisition needs to be parallelised and this is achieved with an FPGA. Six Analog channels are used to sample the phase voltages and currents at a rate of t_s=20 μs (50 kHz sampling frequency). The measured quantities are immediately converted to *dq* domain and are stored in a FIFO buffer. For a 50 Hz power system, the corresponding time period of 1 cycle is t_{sys}=20 ms. The number of cycles *N* that should be within the data acquisition (DAQ) phase is subjective to experimentation. In this deliverable, the DAQ phase is active for *N*=10 cycles i.e. for 200 ms. The size of FIFO buffer and data volume is dependent on the sampling time period (which is also the noise injection time period) and the number of cycles *N* by the following relationship.

$$N_s = \frac{N \cdot t_{sys}}{t_s} \tag{2.2}$$

2.3.3 Impedance Calculation and Estimation

2.3.3.1 Fast Fourier Transform (FFT)

The time domain *dq* voltage and current data are converted into the frequency domain using the FFT subroutine and a Hanning window is used to weight the measured samples to minimise spectral leakage.

2.3.3.2 Non-Parametric impedance calculation

The non-parametric impedance can be calculated by dividing the FFT of the voltage with the FFT of the current. In order to cancel out harmonics introduced by the switched converter, a cancelling routine is introduced. For a short time-frame, the voltage/current data is recorded when the PRBS is not injected to get the floor noise introduced by the switching converter. The corrected voltage/ current spectrum is obtained by subtracting the spectra without injection from the spectra during injection. The assumption is that these spectra do not change during the short time frame and external factors are not involved. The non-parametric impedance calculated from this routine will be devoid of any switching harmonics introduced by the converter itself. We perform a test with an impedance model which is mathematically modelled and known a priori shown in red in **Figure 2-5**.

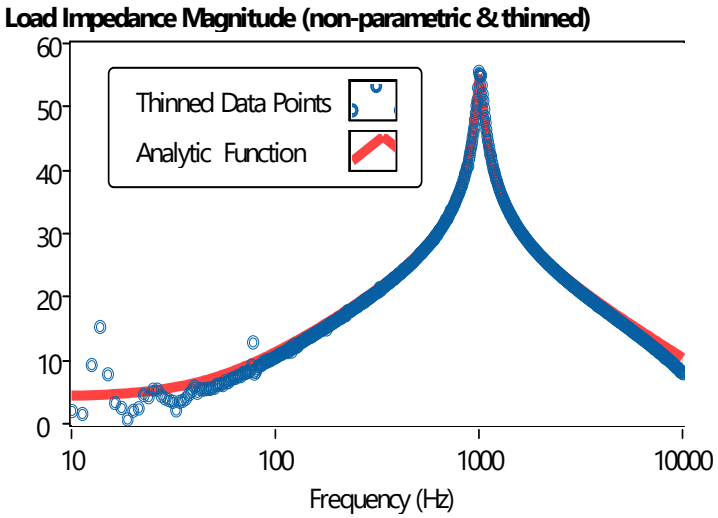

Figure 2-5 *HiL* test for validating the Labview WSI tool with an analytically known grid impedance model

2.3.3.3 Parametric impedance: Linear System Identification approach

Due to inherent non-linearities, there could be cross band frequencies which might affect the performance of identification. For this purpose, data thinning is done by equally weighting the frequency domain data to obtain a logarithmically spaced subset of the data points. Linear system identification technique based on complex curve fitting is applied to determine the parametric impedance model. The order of numerator *n* and denominator *m* must be selected prior to the estimation. Labview implementation is carried out using “Mathscript Node”, which allows including MATLAB code to be executed on the LabVIEW Real-Time Host PC.

2.3.4 Performance of the WSI tool

Due to the heavy computation in the impedance calculation and estimation part, the real time performance of the WSI technique needs to be understood for practical implementation on field. The complexity of the FFT algorithm is O(N·log(N)) and the execution times of system identification depends on the exit conditions. The overall computational time of impedance estimation and calculation is about 20 ms. If the PRBS injection window is roughly 10 cycles or 200 ms, then the overall computation time is 220 ms.

Apart from the nonlinear dynamics of the system which are already mentioned, one of the most interesting challenges is the impact of the inverter filter. An LCL filter has a slope of -60db/dec past its cut off frequency. The cut-off frequency of the LCL filter is usually designed to be one tenth of the switching frequency. Therefore, the grid impedance estimation past one tenth of switching frequency becomes challenging. The spectrum of the PRBS noise should be reshaped to compensate for the filter effect. Typically, a noise whose amplitude is proportional to the frequency (such as blue noise) can compensate for this effect.

2.4 Simulation and *HiL* Results

2.4.1 HiL setup

The proposed HiL setup is generically shown in **Figure 2-6**. The PRBS generator, data acquisition and impedance calculation routines are implemented in LabVIEW. The multi-threaded architecture of Virtex-5 programmable FPGA of the NI PCIe-7841R RIO platform enables the parallel operation of PRBS injection and data acquisition. The high-performance DAC and ADC for the outgoing and incoming data conversion aids the process. The impedance calculation and complex curve fitting is also a computationally complex process which is performed with ease

using this hardware. The input to this simulation environment are the voltage and current measurement data, and the output is the PRBS signal.

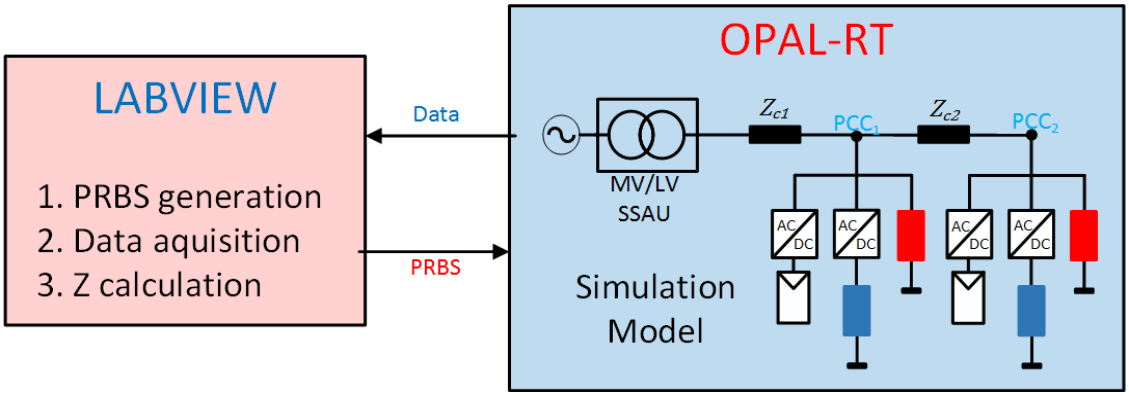

Figure 2-6 HiL Setup

The RT-Lab environment of OPAL-RT system provides the link to MATLAB Simulink. This allows detailed switched models of grid connected inverters built in MATLAB Simulink to be transferred to the RT-LAB environment, where the complex system can be simulated in a real-time manner with feasibility of real time multiple inputs and outputs. The eMEGAsim open real-time software component of the RT-Lab runs on the OP5600 hardware, which consists of two six core Intel CPUs and a Xilinx Virtex 6 FPGA board. This advanced feature allows complex simulations to be run on real time. This allows the distribution grid model with inverters and active rectifiers from MATLAB Simulink to be loaded into RT-LAB for real time simulations. The input to this simulation from the external world is the PRBS signal and the output is the voltage and current values. For our test, the simulation is executed with a time step of 1 µs.

The PRBS signal can be injected on command using a virtual PC. In parallel, the data acquisition event takes place. The data is that of voltage and current measurements at the output terminals of the inverter model. The time window of PRBS injection, the amplitude of noise and some additional parameters related to PRBS generation algorithm can be varied. In this simulation, the cycles number N=10 and the data acquisition is done at t_s=20 µs.

The WSI tool can be easily integrated as a software component to the controller hardware of the converter.

2.4.2 *HiL* Results

For testing the WSI tool, we consider two types of grid.

Case 1: A passive/ conventional distribution grid with no other inverters except our test inverter. All loads in the grid are passive RLC load.

Case 2: Additionally to Case 1, we consider the presence of another inverter in the grid forming a tightly coupled system with possible harmonic stability issues and multiple resonance due to the differently tuned control bandwidths.

Upon initiation of the DAQ in the Labview WSI tool, a PRBS noise signal is injected at the rate of 50 kHz for 10 cycles of the power system frequency, i.e. between 0.2 to 0.22 seconds as seen from Figure 2-7 and **Figure 2-8**. The noise is injected in the control signal of the inverter, at first in the *d*-axis. The *HiL* experiment is repeated for noise injection in *q*-axis of control signal.

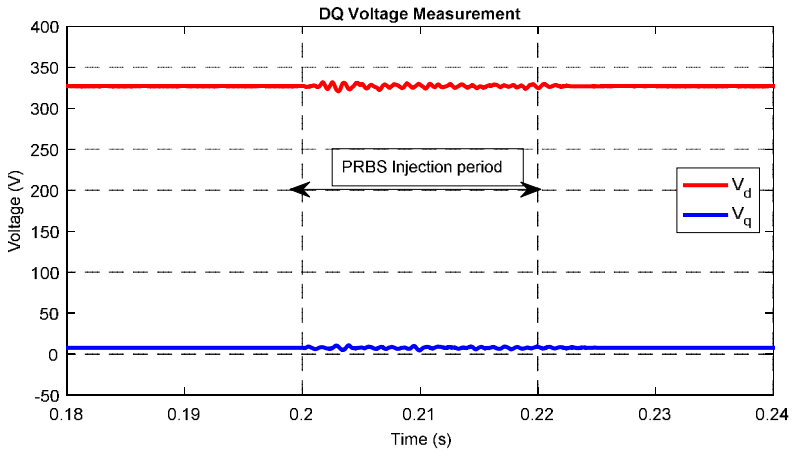

Figure 2-7 DQ Voltage waveform during PRBS injection

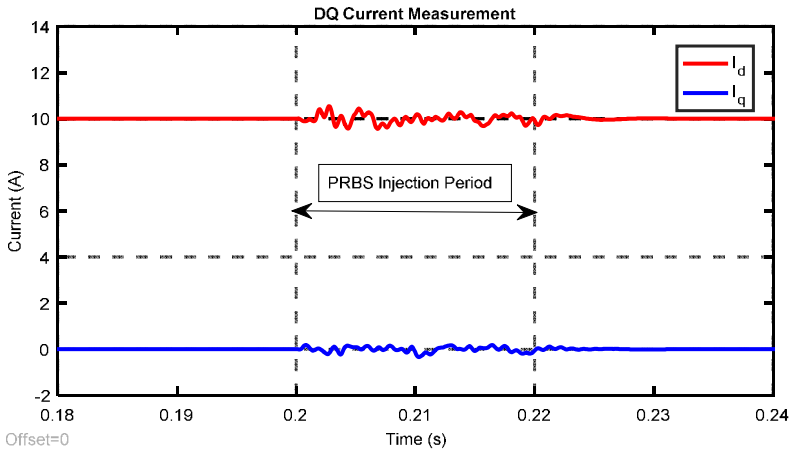

Figure 2-8 DQ Current waveform during PRBS injection

2.4.2.1 Case 1

In this scenario, we consider a passive grid impedance which is unknown a priori. The WSI tool firstly extracts the non-parametric grid impedance followed by which linear system identification technique is applied to determine the parametric impedance. The extracted *dq* matrix is represented by 4 frequency domain plots where the diagonals represent Z_{dd} and Z_{qq} impedances and the off-diagonal plots represent Z_{dq} and Z_{qd}. Results of this test case is shown in **Figure 2-9**. By a rule of thumb, we know that for a given sampling frequency, the maximum frequency which can be captured effectively without distortion is roughly one sixth of sampling frequency although theoretically according to Nyquist theorem, it is possible to observe one half the switching frequency. Therefore, our observation window is up to 10 kHz.

The order of the system to identify is fixed as 4 by experimentation. Future work will be to make the order determination in an adaptive manner.

Both the diagonal and off-diagonal elements are identified accurately. At higher frequencies, there exists distortion in the measurement of off-diagonal impedances. The reason is that the controller of the inverter has decoupling control loops which try to minimise the effect of coupling. Hence there is very strong disturbance rejection properties associated with the inverters controller. From the frame of reference of the controller, the injected noise in the control signal is like a disturbance which is strongly rejected at higher frequencies.

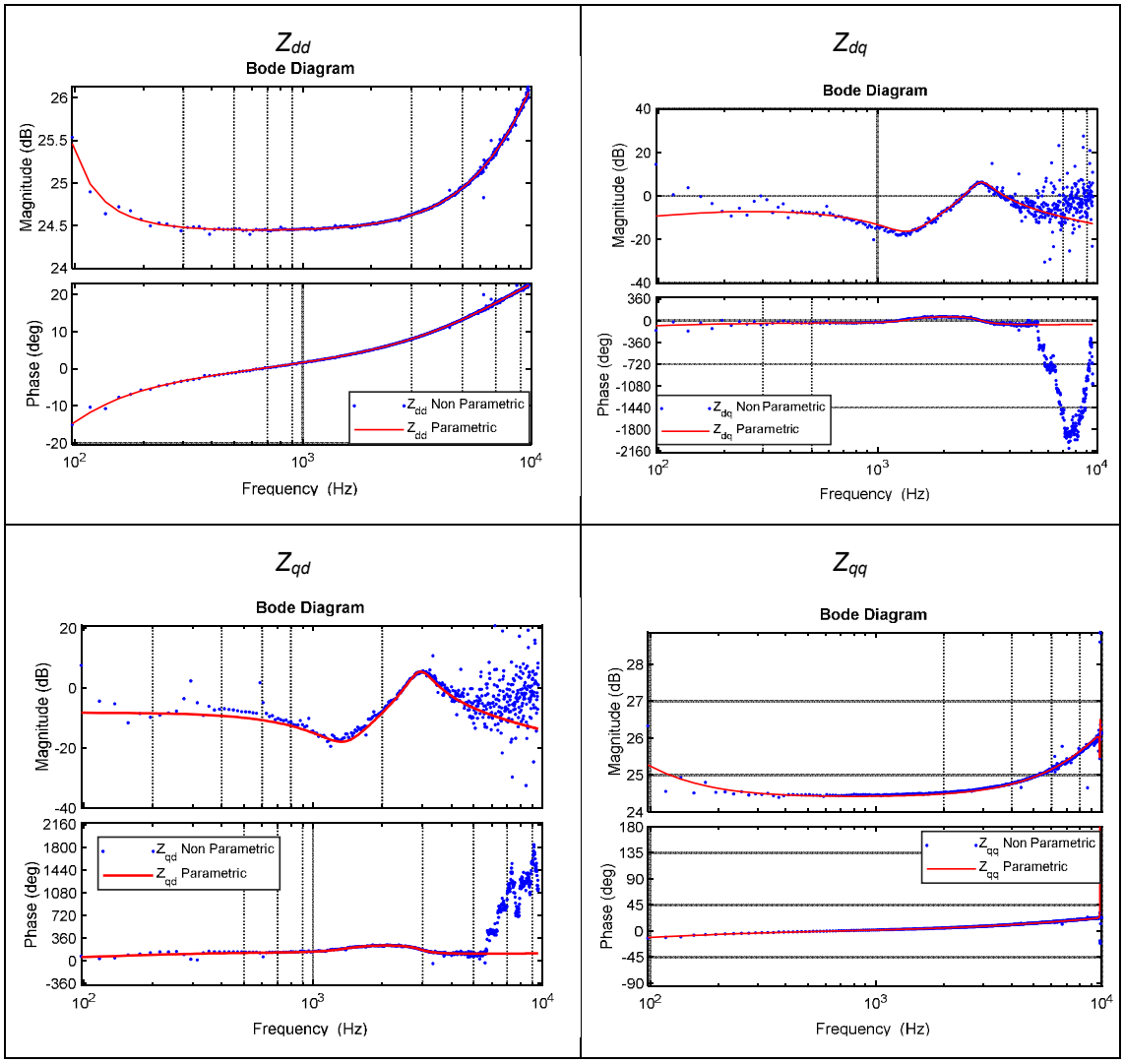

Figure 2-9 Validation of WSI in a Passive Grid

2.4.2.2 Case 2

An identical test is performed as in the previous case, but the grid model now contains active components such as power electronic converters. The impedance identification results are presented in **Figure 3-1**. **Figure 3-1** clearly elucidates the multiple resonance phenomenon in active distribution grids which could lead to harmonic instability issues. One can observe resonances occurring at 1.8 kHz and 6.5 kHz.

The order of the system is chosen as 4 and the identified parametric grid impedance model fits the non-parametric model accurately. Here again due to the strong rejection of cross coupling terms in the control, the off-diagonal estimation is affected at higher frequencies. The test with an active grid impedance model shows that the developed WSI tool is very robust and accurate. Conclusions drown in these studies are presented in section 4 along with the main concluding remarks of the next chapter.

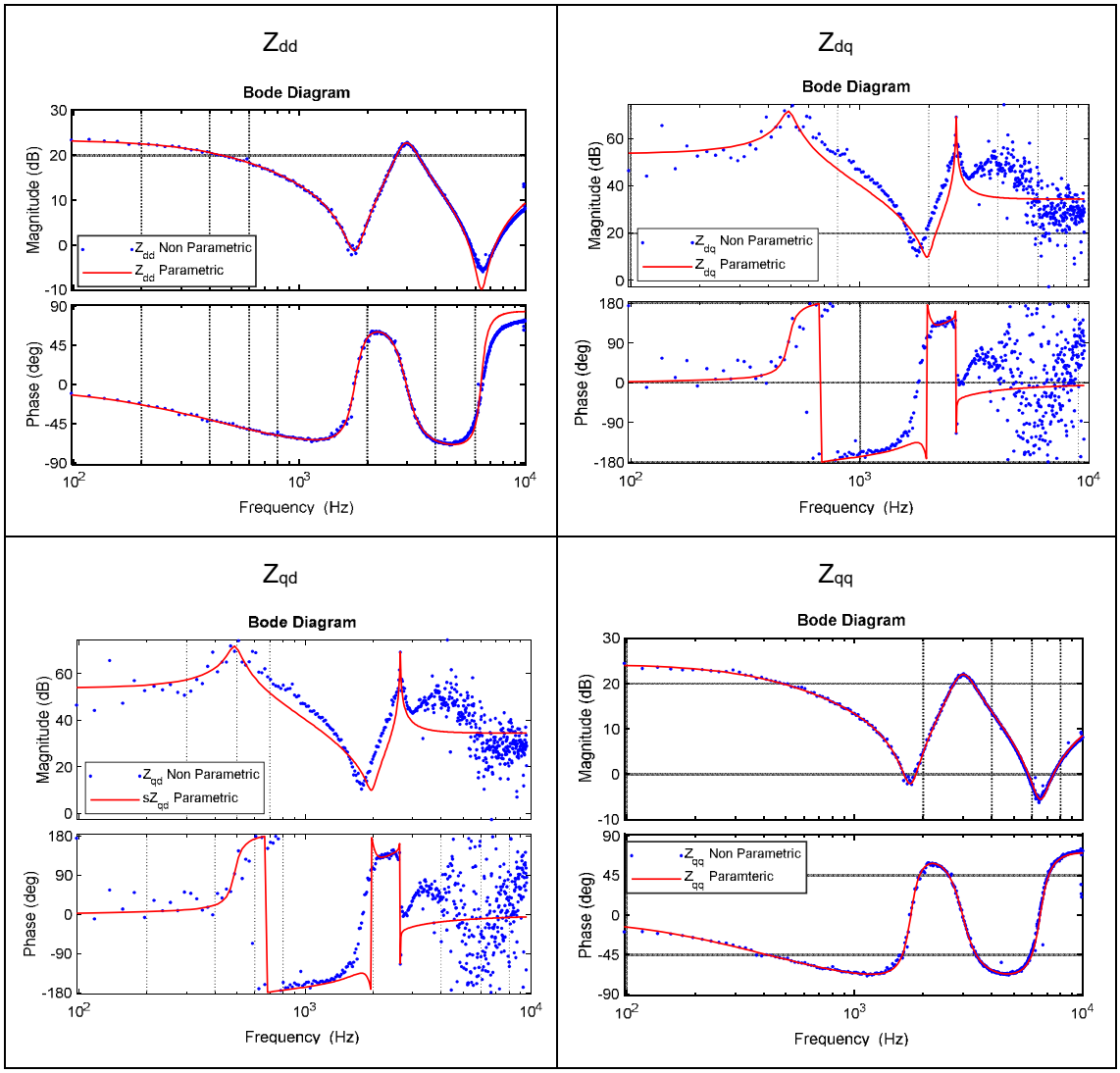
Zdd
Bode Diagram
Magnitude (dB)
Phase (deg)
Zdd Non Parametric
Zdd Parametric
Frequency (Hz)
Zdq
Bode Diagram
Magnitude (dB)
Phase (deg)
Zdq Non Parametric
Zdq Parametric
Frequency (Hz)
Zqd
Bode Diagram
Magnitude (dB)
Phase (deg)
Zqd Non Parametric
sZqd Parametric
Frequency (Hz)
Zqq
Bode Diagram
Magnitude (dB)
Phase (deg)
Zqq Non Parametric
Zqq Paramteric
Frequency (Hz)

3. Figure 3-1 Validation of WSI in an Active Distribution GridImpedance-Driven Static Voltage Control

3.1 Introduction

A novel method was proposed in this work package for voltage management in unbalanced distribution systems with high penetration of inverter-based controllable devices, e.g., PV arrays, V2G systems, controllable wind turbines, and energy storage systems. This high penetration leads to both new challenges (such as voltage profile violation and reverse power flow), and also new opportunities for control and management of these systems. The proposed active voltage management (AVM) algorithm sits in the SSAU. Inputs to the proposed AVM algorithm are presented in Section 3.2. Outputs of the algorithm: reactive power support provided by the inverter-based and the available capacity of active voltage control.

In **D3.2** and **D3.3**, the basic foundations of the proposed decentralized active voltage management and the practical limitations that should be considered in the operation of the system controllable devices were discussed, respectively.

According to **D3.3**, one of the main factors that affects the Volt-var curves in a three-phase unbalanced distribution system is the system configuration, i.e., the network configuration and also availability of the system controllable devices. It is quite possible that in operation of a distribution, the system configuration is changed due to electrical faults, scheduled maintenance, forced outages of the system components and also operation strategies. These may drastically change the most important parameter in the VVCs assigned to each inverter, i.e., the intercepts of the VVCs. According to **D3.3**, these intercepts are approximately equal to the target voltages at PCCs of the system inverters which are the voltages that the system inverters are assigned to follow under voltage control mode of operation.

The impedance identification technique can be considered as an option to develop a more accurate and effective Volt-var optimisation scheme. A VVO framework is developed which also apply this technique to find out whether or not such technique can be applied. In this chapter, the effects of the network configuration and also the availability of the system controllable devices on the proposed active voltage management algorithm are analysed.

The rest of this chapter is organised as follows. The data required for the offline calculations and also the online implementation of the proposed AVM technique are listed in Section **3.1**. The proposed AVM algorithm to consider the effects of the system configuration on the results of the offline calculations in order to extract the VVCs is presented in Section **3.3**. The results of the offline an online studies are presented in Section 3.4 in order to extract the VVCs in different system configuration and to validate the effectiveness of the proposed active voltage management algorithm. Finally, the concluding remarks are presented in Section **4** based on the results of the case studies of this chapter.

3.2 Input data for Volt-var Optimisation (VVO)

The accuracy of the input data and measurements is of utmost importance, and a key factor in extracting a proper Volt-var control scheme for a low-voltage distribution system enabled with inverter-interfaced RESs and also in developing an effective voltage control strategy in each possible future scenario in such systems. In this sub-section, the input data required for extracting the Volt-var curves through the offline simulations have been discussed as well as the data required in order to develop the voltage control strategies using the VVCs in online application of the proposed AVM algorithm.

3.2.1 Data Required in Offline Simulations to Find the AVM strategies

3.2.1.1 Network characteristics.

Network configuration should be supplied as one of the main inputs in order to extract the Volt-var control scheme, i.e., the VVCs. Since the networks are usually unbalanced in low-voltage distribution systems, it is necessary to supply the three-phase diagram of the system including

the transformer phasor group, load type (single- of three-phase), load connection type (delta or star), grounding type (grounded or ungrounded) as shown in **Figure 3-2**.

Line characteristics should also be provided as an important input data to the proposed decentralised AVM algorithm. Additionally, the line resistances, self-reactance of each phase and mutual reactance between different phases should be provided.

If there is any type of fixed reactive power compensators (such as capacitor banks) installed across the system network, the technical characteristics of these compensators should be provided in order to extract the VVCs.

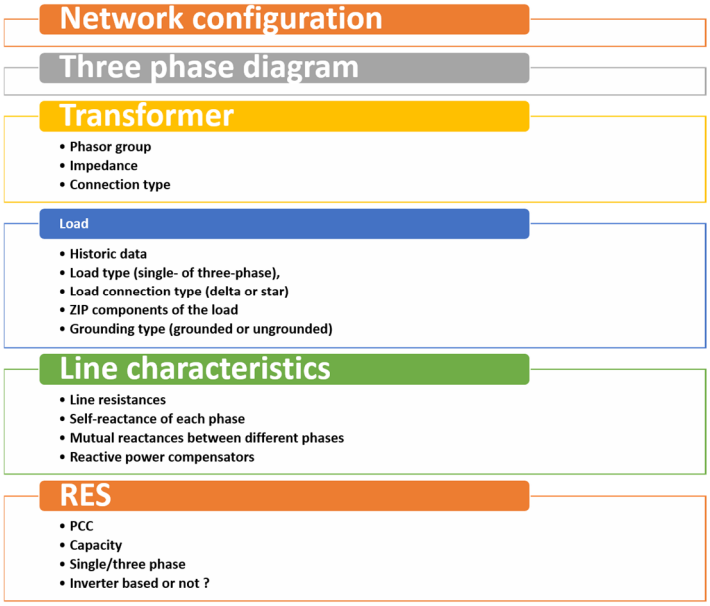

Figure 3-2 Data Required in Offline Simulations to Find the AVM strategies

3.2.1.2 Load characteristics.

The historical load levels at each load point or at least the historical data on the total load level should be supplied as well as the number of customers, load types and load connection at each load point. A change in the load levels at various load points may drastically change the voltage profile and can change the control action required as shown in **Figure 3-2**.

On LV networks, the consideration of *load to voltage sensitivity* is of utmost importance. The voltage sensitivity is an outcome of the physical infrastructure that the network embodies but it is also dependent on the generation and load composition. A bottom-up demand model [16] is used here to construct a representative demand profile of any amount of customers on an LV feeder. This model epitomizes occupancy patterns and behavioural characteristics of the customer to provide a load composition that gives an accurate representation of the devices assumed to be drawing current. Thus, this style of model has the advantage of also including the representative ZIP composition of the customer premises. More information in this regard can be found in **D3.2**. Here, it is necessary to supply the historical load to voltage sensitivity factors.

3.2.1.3 Characteristics of the system inverters.

Maximum capacity of the inverters should be declared. If there are other limitations in operation of these inverters they should also be provided. These practical limitations depend on the inverter type, e.g., solar PV inverters and battery storage inverters. These limitations should be determined to ensure the safe operation of the inverter itself and also to restrict the undesired impacts of the operation of each specific type of inverter on the power quality of the system costumers.

The inverter type (solar, battery… single- or three-phase), connection type (star or delta) and other configuration information of the system inverters should be provided as shown in **Figure 3-2**. It should be noted that some types of inverters cannot be applied to solve/mitigate some

specific problems in a certain type of distribution system. **Table 3-1** shows the objectives that can be selected to be followed according to the type of the inverters and also the network. In the active voltage management of low voltage distribution systems, the main objective depends on the system needs and also availability of the controllable devices that can effectively satisfy such objectives. In such systems, availability of renewable energy resources and other controllable inverter-interfaced devices enables the system operator to control the load point voltages more effectively to achieve a variety range of objectives. In this project, three main objectives are considered for the active voltage management in futuristic low voltage distribution systems. These objectives are presented in **Table 3-1**.

Table 3-1 Objective menu

Code	Objective	Requirements	Three phase Network	Single phase Network
1	Voltage unbalance improvement	Single-phase inverter	✓	X
2	Loss reduction	Both Single/three-phase inverters	✓	✓
3	Improvement of voltage deviation ($V_{desired}$=1 pu.)	Both Single/three-phase inverters	✓	✓

Historical data on the energy generation of RESs should also be provided to develop the scenarios of RESs' power production. It is very important that the proposed method embodies a prognosis of the future operating conditions based on the historical data that should be provided as an important part of the impute data for the proposed AVM algorithm.

3.2.1.4 Inverter mode of operation.

Most of controllable inverters are operated under power control mode. i.e., the value of active and reactive power injections are set by the system operator. Some other controllable inverters are operated under voltage control mode. The operation mode of each inverter should be determined in order to develop the proper voltage strategy that can be applied to each specific inverter. Moreover, under both of these operation modes, the inverter limitations should be taken into account (see **D3.3**).

The active voltage management includes different control modes for the inverter-based resources to optimise their performance depending on whether the generator is connected to the grid, or is in island mode. Therefore, they can be set to maintain the voltage (voltage control mode), the PF (power factor control mode) or the reactive power (power control mode).

In this chapter, the extracted VVCs are applied to find the optimal reactive power set-points in power control mode of operation. In the process of extracting the VVCs, an optimal voltage is found for each inverter (see subsection 3.3.1). It should be noted that the optimal voltages can be considered as the voltage set-points in the voltage control mode of operation for these inverters. If the inverters follow these voltage set-points in the voltage control mode of operation, the results will be the same as those that are obtained in power control model of operation where the inverters are tasked with following the reactive power levels that are found using the extracted VVCs. In fact, in both control modes of operation, the inverters should try to follow the optimal voltages as accurate as possible based on the operational limitations which should be considered for each type of inverters.

3.2.1.5 Operator Objectives.

Different objectives can be considered for voltage control in low-voltage distribution system (**Table 3-1**), e.g., minimisation of voltage unbalance, minimisation of active power losses and minimisation of active and reactive power purchase cost. The voltage control objective should be declared by the system operator.

Selecting the proper objective function depends widely on the issues faced that the distribution system operator is faced with and also the type and capacity of controllable devices that can be controlled to achieve a specific objective. As an example, in a low voltage distribution system with only one small single phase battery inverter installed on phase *a*, there is not enough control

capacity to improve the average value of the phase voltages at system three-phase load point. **Table 3-1** gives an insight into the types of the objectives that can be considered in different circumstances.

3.2.1.6 Inverter impedance as a function of frequency (viewed at the connection point of each inverter).

A framework is developed in this chapter to consider the impedance identification technique (proposed by SV_A (AVM)) to improve the voltage control effectiveness in SV_B (DVSM/VOIP). The details of this framework are discussed in subsection **3.3**.

The grid-tied inverter output impedance (the inverter impedance viewed from the connection point shown in the **Figure 3-3** by $Z^{network}$) of each inverter-interfaced RESs available in the system should be provided as a part of data required in extracting the VVCs. In this figure *w* is the angular frequency.

However, the practical requirements of applying the impedance identification technique are not yet available in the practical low voltage distribution systems. This chapter provides the theoretical foundations of the decentralized technique to develop the adaptive control strategies based on the system configuration approximated according to the identified impedance at inverter PCCs. A supervised closed loop decentralised voltage control approach will be developed in **D3.5** to cope with the shortcomings of the proposed technique provided in the present chapter of this deliverable. The supervised control technique solves the problem associated with the absence of the up-to-date identified impedance or the potential errors that may occur in the impedance identification process.

For more information regarding the adaptive AVM algorithm presented in this chapter based on the impedance identification technique, please see subsections 3.2.2.4 and 3.3.

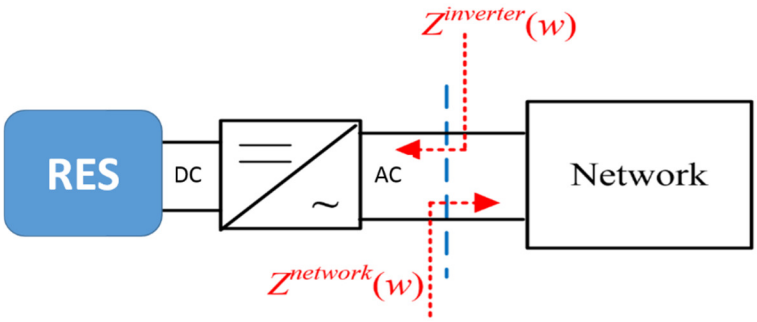

Figure 3-3 Inverter and network impedances.

3.2.2 Data Requirement in Online Application

After extracting the proper decentralized control scheme, e.g., Volt-var Curves, it is necessary to measure some local parameters and transfer the measured values to the local control unit, in order to develop the proper control strategy, i.e., reactive power support of the inverter-interfaced RESs in application stage. Here the data required in order to find the reactive power support provided by each inverter-based RES is outlined.

3.2.2.1 Voltage at inverter connection point for each RES

At each connection point, the value of 3-phase voltage should be measured (before finding the optimal reactive power support of each inverter) and transferred to the local control unit (see **Figure 3-4**). For single phase controllable inverters the data on the voltage levels of other phases may be unavailable. For these inverters there is no other choice except for measuring the single-phase voltage and developing the control strategy based on this measurement.

3.2.2.2 Active and reactive power injection of the inverters before developing the voltage control strategy.

The capacity of each inverter is limited by the maximum current that the device switches can interrupt or the thermal current limit specified by the manufacturer and also by the maximum

inverse bias voltage of the switches or the maximum voltage level that the device insulation can tolerate in steady state condition [17].

In the steady state studies of power systems, these limitations are usually modelled by a single constraint, i.e., the apparent power injected by this inverter cannot be higher than the maximum allowable apparent power which is always referred to as the inverter capacity. In **D3.3**, it has been discussed how to consider this limitation in AVM algorithm. There may be some other limitations that depend on the inverter type. The next subsection briefly discusses these limitations. More information can be found in **D3.3**.

3.2.2.3 Additional limitations of the inverters.

For some PV units, it is necessary to consider the maximum power angle (regarding minimum permissible power factor) to avoid high harmonic distortions. Such limitation imposes new upper bound for the change in the reactive power support which should be treated in the same way as the upper bound regarding the maximum capacity constraint. Fortunately, in most of low-voltage distribution systems, the harmonic limitations are not very tight. However, if there is any limitation in the operation of system inverters, these limitations should be considered in developing the voltage control strategy which determines the reactive power support of each inverter especially in futuristic distribution network with high penetration of RES.

For different systems, if there are such limitations, they should be declared to be considered in extraction of the VVCs and also in the final function which is developed for online application of the proposed VVO based on the extracted VVCs (see **Figure 3-4**).

3.2.2.4 Network impedance viewed by the inverter from the connection point (in the main system frequency and some selected frequencies if possible).

In the project definition, the impedance identification technique can be considered as an option to develop a more accurate and effective VVO scheme. In this chapter a VVO framework which apply this technique to find out whether or not such technique can be applied.

In the decentralized control system, it is assumed that the local control agent has no information about the other controllable devices installed at other connection points. The main goal of measuring the system impedance at each connection point ($Z^{network}$ in **Figure 3-3**) is to identify or approximate the characteristics of the system, e.g., system configurations and also the availability of the inverter-interfaced controllable devices installed at other connection points in this system (see **Figure 3-4**).

Usually, the small systems with one or two inverter based controllable devices have fixed configurations and therefore, the impedance identification technique [18] is not applied on these systems. Moreover, the practical requirements of applying the impedance identification technique are not yet completely available in any practical low-voltage distribution system. Therefore, in order to accomplish the items determined for Task 3.4 in this work package, this technique is implemented in this chapter where the simulations are conducted based on measuring the network impedance viewed from the connection point of the inverters to see whether or not this technique can be applied to improve the effectiveness of the proposed VVO framework developed as a part of SV_B voltage control plan. A real size distribution system will be considered to test this technique.

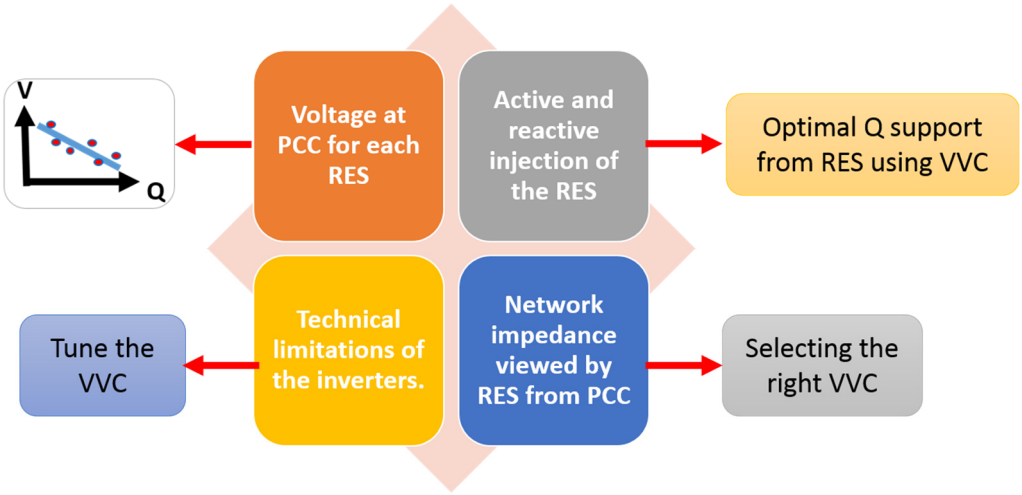

Figure 3-4 Data Requirement in Online Application

3.3 Extension of AVM to consider different contingencies which influence the network impedance seen by PCC

3.3.1 Summary of the Proposed AVM Algorithm Proposed for a System with Fixed Configuration

The basic proposed active voltage management is a decentralized algorithm for active voltage management to maintain the steady state voltages in the presence of different inverter-based RES technologies. The proposed technique controls the provision of reactive power from these units using an optimisation method.

An offline network analysis is conducted as a centralised solution which is briefly explained in this section. More details of the basic decentralised AVM algorithm can be found in **D3.3** and **D3.3**. The method of obtaining and applying the Volt-var Curves (VVCs) for voltage control is outlined below and depicted in Figure 3-5:

- Stage 1: determines the optimal voltage across all scenarios that minimises the voltage unbalance of the feeder, or other objectives of interest, considering unlimited reactive power support for all RESs.
- Stage II: determines the closest possible voltage deviation from optimal in each scenario, constraining the reactive power of the RES units to within representatively realistic bounds.
- Stage III: the voltage levels without any changes in the reactive power injections of the controllable devices, i.e., base voltages, are found.
- Stage IV: to conclude the offline-procedure the resulting reactive power set-points (Stage II) are plotted against the resulting voltage set-points (Stage III) to determine the Volt-var curves for each RES system.
- • In application mode, for each inverter, the voltage is measured at PCC and the value of the change in the reactive power injection is found using the regarding VVC. The value of the final reactive power injection of this inverter is found according to its capacity and other operational constraints.

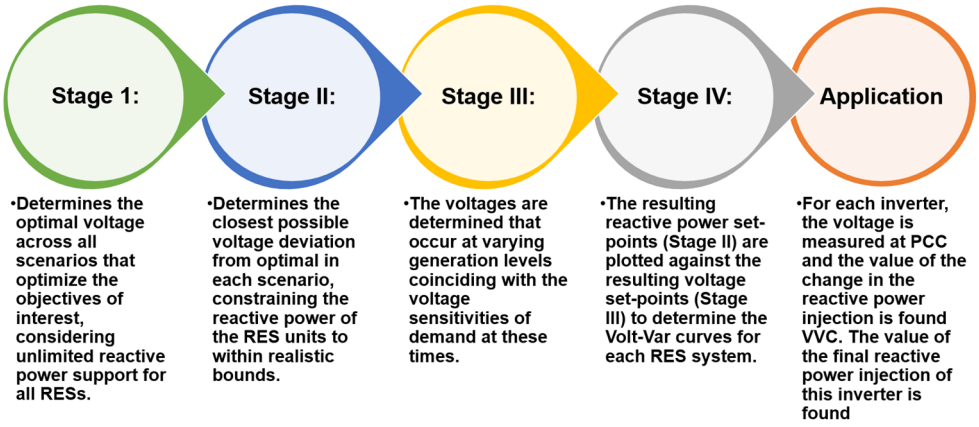

Figure 3-5 Method of obtaining and applying the VVCs for voltage control

In most of the practical applications, a simple power factor limit, e.g., power factor>0.95 lag, is still being used as the industry common engineering practice for reactive power control of the inverter based controllable devices. In this subsection, first, it has been discussed how these new operational constraints (which are mostly proposed for safe operation of RESs as well as achieving higher levels of power quality) affect the voltage controllability in low voltage distribution systems enabled with different types of controllable devices comparing to the industry common practice (power factor limitations).

The proposed AVM in **D3.2** and **D3.3** is based on the fact that all inverter-based RES units are in normal operation and the Thevenin model of the network seen from the PCC of each RES remain unchanged. As it is expected in reality, some network topology might change due to the failure of some components which alters the basic assumptions of the proposed AVM. This chapter intends to propose a Resilient Active Voltage Management (RAVM) to remain robust against possible RES failure events.

3.3.2 Influence of network characteristics on AVM

In futuristic distribution networks, there might exist several RES technologies at different PCCs. The Thevenin equivalent of the network seen by each individual RES is different and depends on the network characteristics and also the behaviour of other RES in the network [19] as shown in **Figure 3-6**.

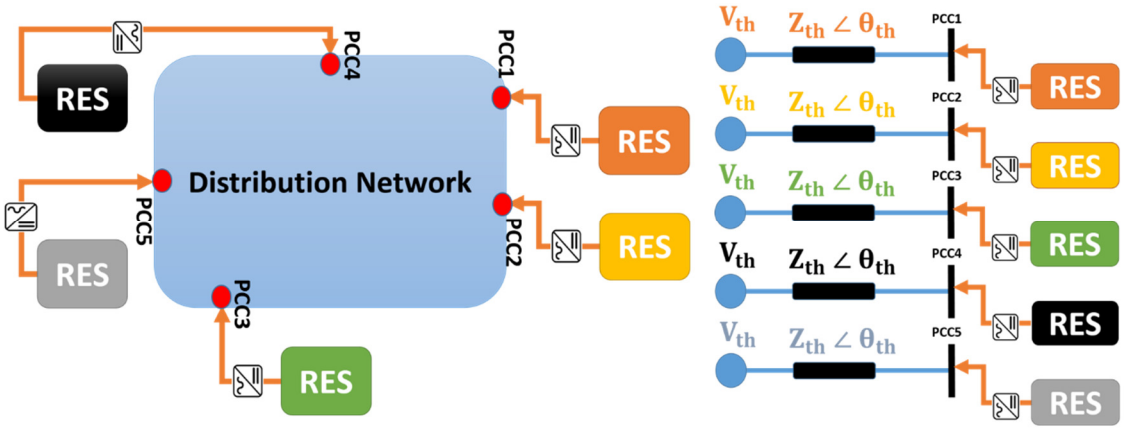

Figure 3-6 Schematic of network seen by each individual RES

The Thevenin network seen by each RES is dependent on several parameters such as those as described in **Figure 3-7**.

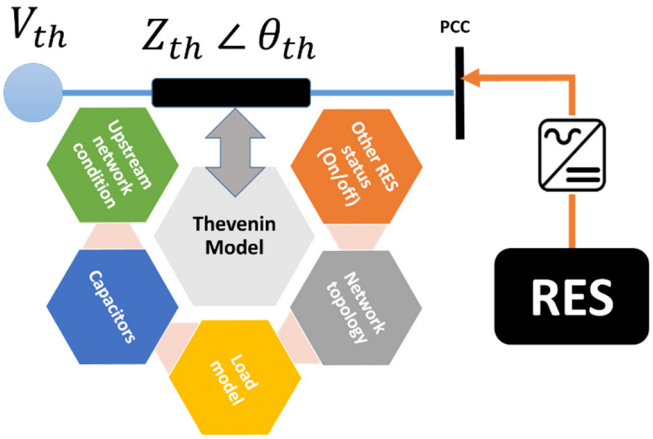

Figure 3-7 Factors influencing the Thevenin network equivalent seen by each RES from PCC

The impact of network parameters as well as the demand characteristics on VVC are already captured in operating scenarios described in **D3.2** and **D3.3**.

3.3.3 Network component failure

The VVC of each individual RES is obtained and used for active voltage management as described in **D3.3** and **D3.5**. The idea of VVC is based on the fact that the equivalent Thevenin model of the network seen from PCC of each RES does not change. In reality, many factors might cause changing the equivalent Thevenin model seen by each RES. This will deteriorate the effectiveness of the designed AVM. The influence of the RES/inverter failure of AVM performance is shown in **Figure 3-8**.

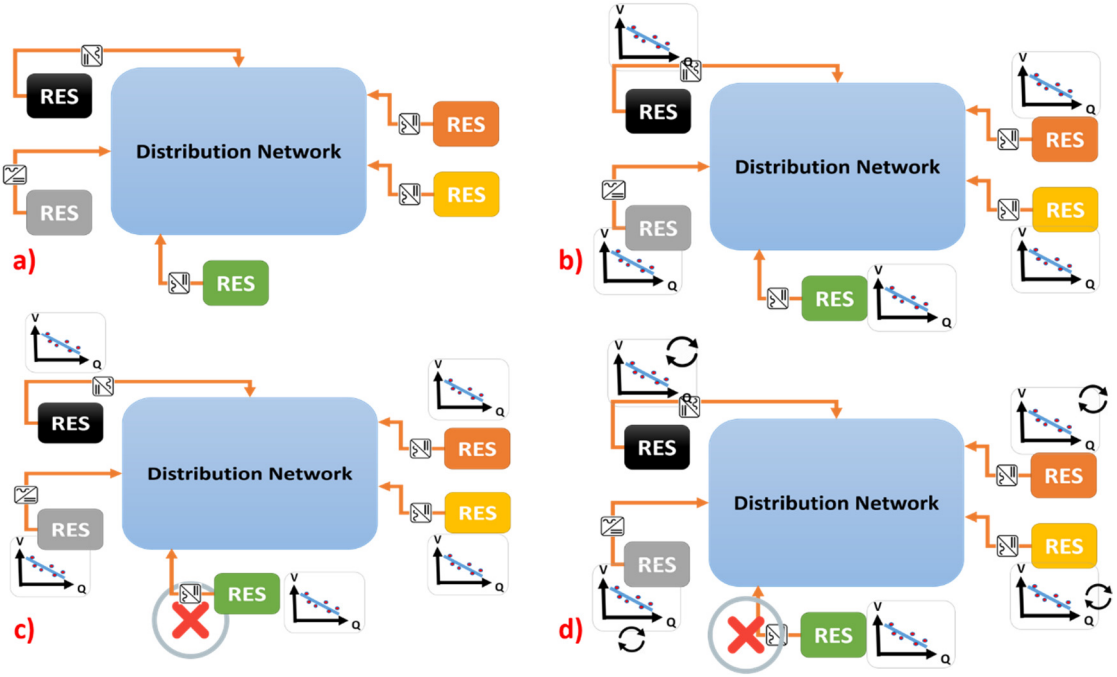

Figure 3-8 Influence of the inverter/RES failure on AVM performance

- Figure 3-8-a) Shows the futuristic distribution network with several inverter based RES connected to the grid. These technologies can be of PV, wind, storage or any inverter based energy resources.

- Figure 3-8-b) Shows the same futuristic distribution network that for each individual RES, a VVC is tuned and optimised for the selected objective function using the technique described in **D3.2**.
- Figure 3-8-c) Shows the case when there is a contingency on one of the RES units. In this case, the pre-tuned VVC may not able to provide the required performance. This is due to the fact the Thevenin parameters of each RES (see Figure 3-6) are changed and the VVC is no longer valid for the updated network topology
- Figure 3-8-d) In this case, if there is any contingency on any of the RES,
  - ❖ Initially, the contingency is identified for each RES using a local impedance identification technique (see Section 2)
  - ❖ the VVCs for the rest of them will be updated to capture the changes in the network topology.

So the DSO needs an adaptive and resilient AVM technique to remain robust against the contingencies that might happen to the inverter based RES units. The framework for VVC extraction in resilient AVM method is shown in **Figure 3-9**.

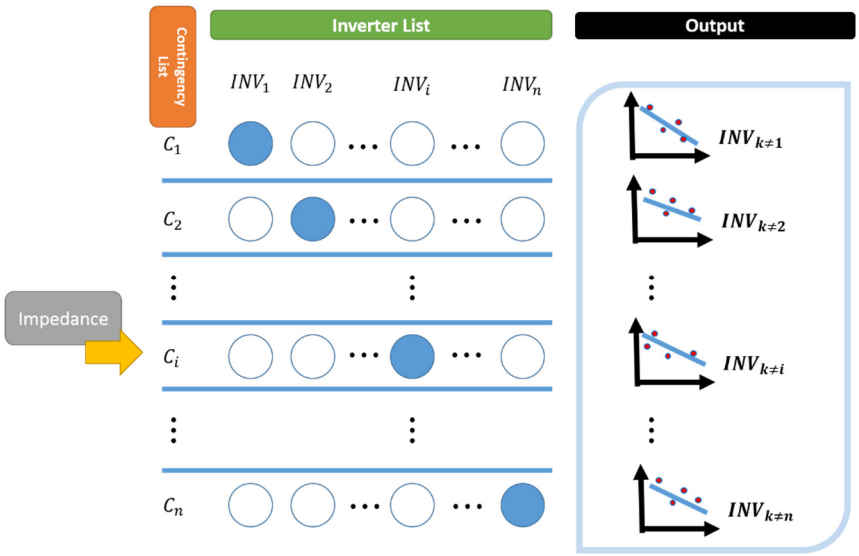

Figure 3-9 Schematic resilient VVC determination for AVM

The following assumptions are taken into account to obtain the resilient set of VVCs:

- The only contingency considered in this framework is the failure of the inverter based RES units
- Only single contingencies are captured in this framework since the probability of simultaneous contingencies with higher orders (two or more components fail at the same time is a very rare event)
- Assuming that there are 'n' RES units in the grid, the VVC extraction is repeated n times.
- At contingency row *i*, it is assumed that the inverter at RES *i* is failed and is not able to inject power to the grid. The VVCs for the rest of the units are optimised.

Once the VVCs shown in **Figure 3-9** is found then the utilization of the RAVM is straight forward. The algorithm described in Section 2, is used to find the impedance seen from PCC of each RES. This impedance can indicate that which row of **Figure 3-9** should be used for selecting the appropriate VVC.

3.4 Simulation Results

In this subsection, the results of applying the supervised decentralized voltage control is presented, when some of the controllable devices are not available during some proids. These

will affect the optimal control strategies. The simulation is done on the sample three-phase unbalanced network as shown in Figure 3-10.

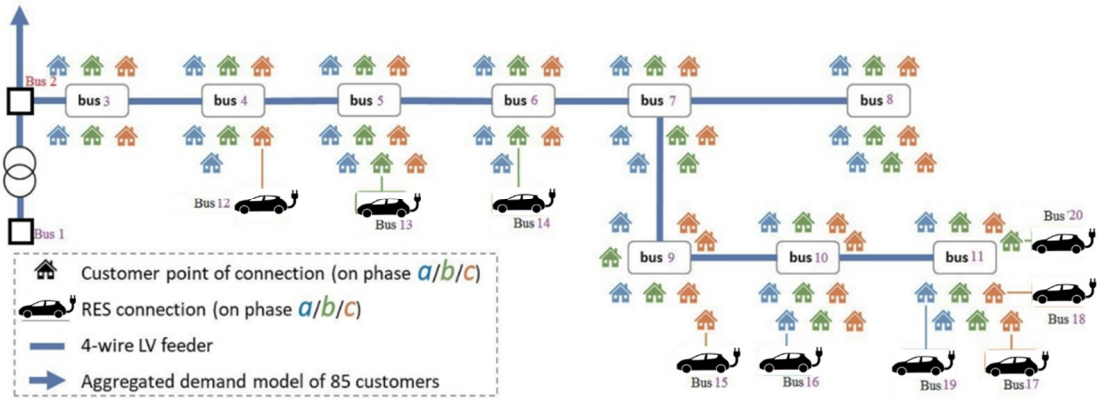

Figure 3-10 Sample three-phase unbalanced network with inverter based V2g

In order to analyse the effects that unavailability of some of the inverters have on the results of the active voltage management algorithm, first the VVCs are obtained in each connection state. A connection state is defined as a vector in which the availability of the controllable devices is specified.

In order to obtain the VVCs in case of the outage of each inverter (or probably a set of system inverters) a centralised offline simulation is conducted. The same steps as those provided in subsection **3.3.1** is followed. For each possible connection state, a set of VVCs are extracted, each of which for a single controllable device.

After extracting the VVCs in each connection state, the results of applying the proposed adaptive AVM technique (which keep the VVCs' characteristics up-to-date whenever the system configuration changes) are compared with those obtained by applying the fixed VVCs which are not changed in varying system configuration.

The proposed adaptive active voltage management technique is tested on the same sample low voltage distribution system as the one which was introduced and used in **D3.3**. This system is a radial LV feeder with 85 nodes situated in Ireland [20]–[23]. The data required for conducting the simulations can be found in **D3.3** and also **D3.2**.

The inverter-based controllable devices which are considered to showcase the proposed algorithm in this subsection are nine inverter-based 2 kVA Vehicle to Grid (V2G) systems connected at different PCCs across the network of this sample system. The data on these V2G inverters can be found in **D3.3**. All the other assumptions were presented in **D3.3**. This makes it possible to compare the results of these studies to those obtained in **D3.3**. Similar to **D3.3**, in this chapter it is assumed that at the head of the feeder in the multi-scenario case, a separate feeder connection off the transformer supplies further 85 customers. The batteries of Electric Vehicles (EVs) have a considerable potential not only to provide energy for the locomotion of EVs, but also to dynamically interact with the low voltage electricity grids.

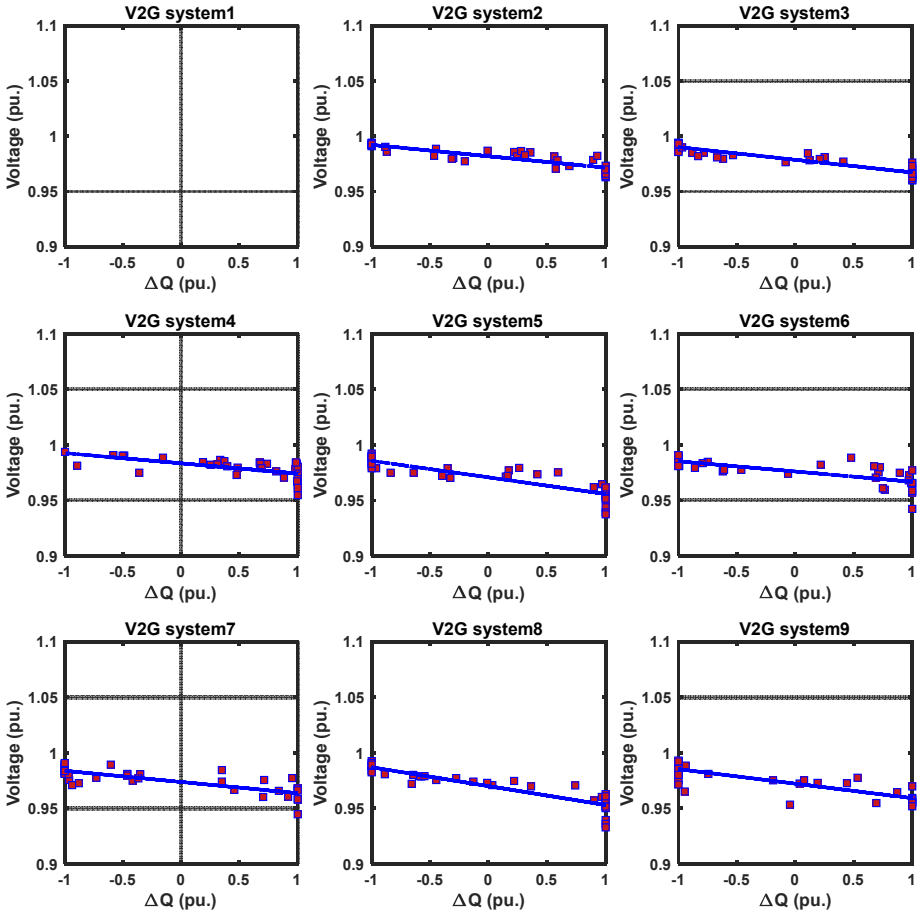

Figure 3-11 Resulting VVCs found for minimisation of voltage unbalance for V2G systems 2-9, showing intercepts and slopes assuming V2G system 1 is unavailable.

It is noticeable that a V2G system typically consumes active power, except for the systems for which both operation strategies and technical characteristics of the charging station allow battery discharge during some periods. The owners of the electric vehicles may also disagree with discharging their vehicles' batteries in the course of time that they left their vehicles to be charged at the charging station. More accurately, the interface between the distribution grid and the electrical vehicles, instead of using typical power converters that only work on unidirectional mode, need to use bidirectional power converters to charge the batteries (Grid-to-Vehicle capability) and to deliver a part of the stored energy in the batteries back to the power grid (Vehicle-to-Grid capability). A collaborative broker is needed to define and control the usage profiles. In that case, it is of utmost importance to take the requirements of the low voltage distribution systems and the convenience of the vehicle owners into account. In the simulations of this section, it has been assumed that the charging station only consumes active power. However, reactive power can be easily exchanged between the V2G system and the grid. In this fashion, the static under-voltage problem may arise as an important phenomenon that needs to be addressed. The active power consumption of the V2G systems may reduce the voltage levels at different load points of the distribution system lower than the values allowed according to the system standards. This necessitates higher levels of reactive power support that should be supplied by the V2G system inverters of the charging stations installed across the network to mitigate the unwanted voltage drop, especially at remote ends. An opposite phenomenon may be observed in distribution systems enabled with PV arrays at different connection points, since the high values of the active power injection (in case of high penetration of the solar production) may cause the voltage levels to rise.

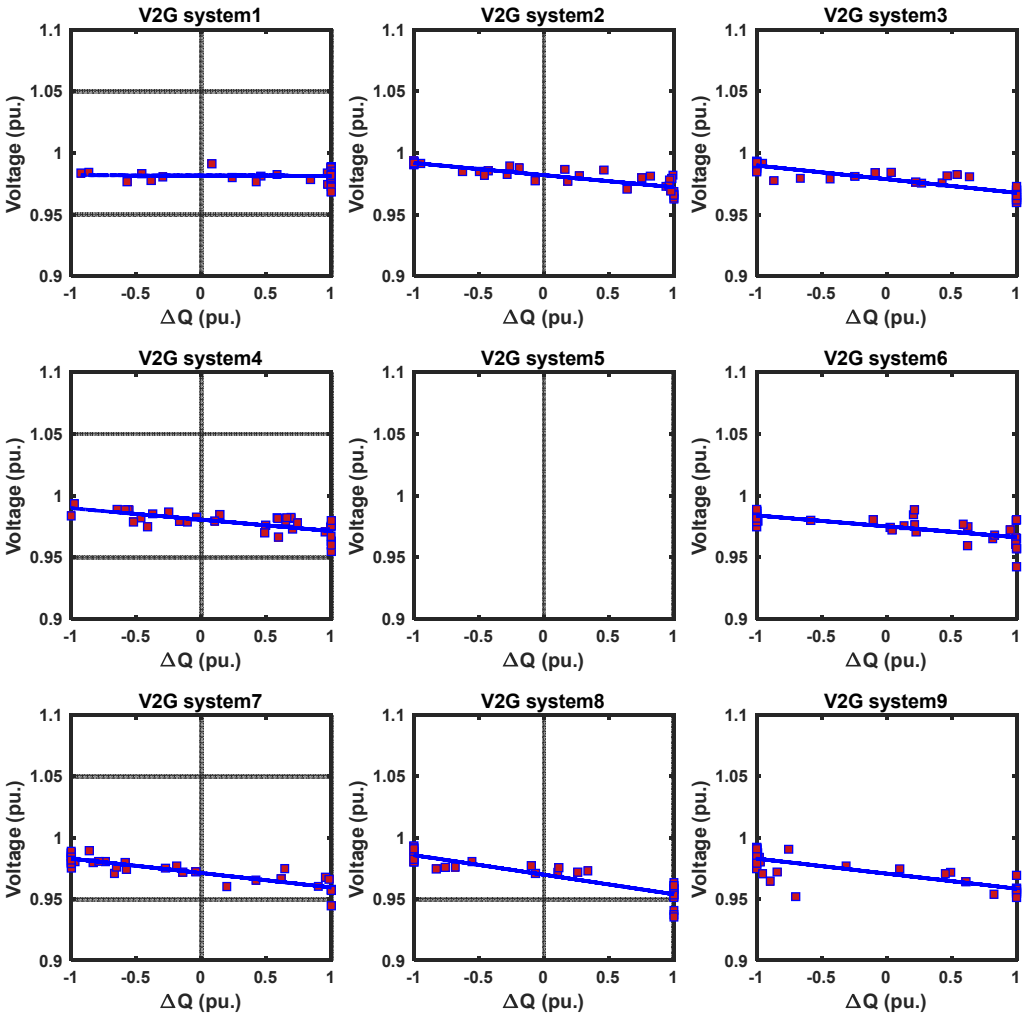

Figure 3-12 Resulting VVCs found for minimisation of voltage unbalance for V2G systems 1-4 and 6-9, showing intercepts and slopes assuming V2G system 5 is unavailable.

In **D3.3**, the VVCs were extracted for this system assuming all the inverters are available. Here, all the V2G systems are disconnected one by one and a set of VVCs are extracted for the system inverters. **Figure 3-11** and Figure 3-12 show the VVCs when V2G system 1 and 5 are unavailable, respectively.

For the sake of brevity, other seven sets of the VVCs, each of which extracted assuming a certain V2G inverter is not available, are presented in A**.1**. **Figure 3-13** shows the optimal voltages found for the remaining system inverters in the case of the outage of each V2G systems. It should be noted that these optimal voltages should be considered as the voltage set-points in the voltage control mode of operation for the available inverters.

If the inverters follow these voltage set-points in the voltage control mode of operation, the results will be the same as those that are obtained in power control model of operation where the inverters are tasked with following the reactive power levels that are found using the extracted VVCs.

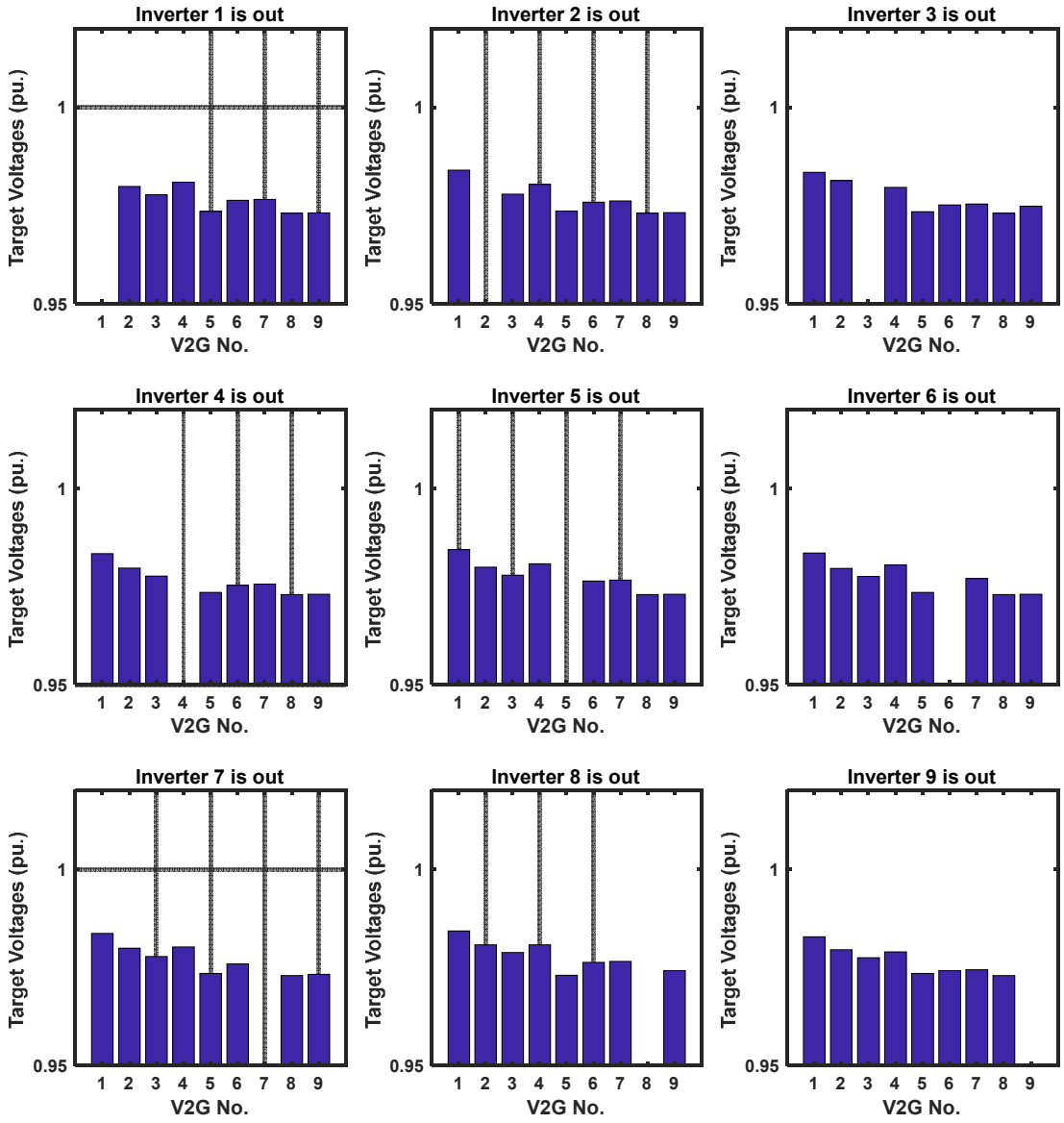

Figure 3-13 Optimal voltage levels of the remaining system inverters at their connection points after the outage of each V2G system

As can be seen in **Figure 3-13**, the optimal voltage levels the PCCs of the system inverters depend on the availability of the other system inverters. This indicates the necessity of developing an adaptive decentralised control scheme like the one proposed in this chapter based on the impedance identification technique. In order to increase the robustness of the algorithm proposed for the active voltage management, a supervised closed-loop decentralised control will be proposed in **D3.5**, where the system configuration is also communicated from a central control unit to the local control systems in a prodigal basis to ensure an accurate system configuration.

Table 3-2 Slopes of the VVCs in each system configuration (m constants for VVCs)

Unavailable inverter	$V2G_1$	$V2G_2$	$V2G_3$	$V2G_4$	$V2G_5$	$V2G_6$	$V2G_7$	$V2G_8$	$V2G_9$
Base case	-0.00120	-0.01043	-0.00939	-0.00793	-0.01368	-0.01145	-0.00935	-0.02598	-0.01178
1	-	-0.01033	-0.01148	-0.00921	-0.01493	-0.00925	-0.01006	-0.01697	-0.01306

2	-0.00079	-	-0.01141	-0.00873	-0.01545	-0.00871	-0.00969	-0.01730	-0.01394
3	-0.00161	-0.00946	-	-0.00930	-0.01565	-0.00961	-0.01102	-0.01741	-0.01244
4	-0.00426	-0.00969	-0.01091	-	-0.01604	-0.00928	-0.00858	-0.01774	-0.01366
5	-0.00020	-0.00983	-0.01106	-0.00923	-	-0.00881	-0.01174	-0.01592	-0.01225
6	-0.00417	-0.01006	-0.01101	-0.00842	-0.01602	-	-0.00828	-0.01696	-0.01349
7	-0.00408	-0.01073	-0.01074	-0.00830	-0.01499	-0.00870	-	-0.01697	-0.01290
8	0.00009	-0.00935	-0.01085	-0.00795	-0.01445	-0.01097	-0.01078	-	-0.01322
9	-0.00291	-0.01009	-0.01022	-0.00859	-0.01602	-0.00828	-0.00958	-0.01766	-

Table 3-2 presents the slopes of the VVCs in each system configuration. As can be seen, all the slopes of the VVCs are negative. This assures a positive reactive power injection when the measured voltages at PCCs are below the regarding target voltages (V_{opt}) and a negative reactive power injection (positive absorption) when the measured voltages are higher than the target voltages. This validates the successful application of the proposed active voltage management algorithm in all system configurations. This is as expected as under steady-state and stable operation (static voltage control), an injection of reactive power to the PCC will raise the voltage magnitude at this location. Similarly, a reactive power absorption at PCC reduces the voltage magnitude. Under this setup, the voltage at each PCC will always follow the regarding optimal voltage. In **D3.5**, a closed-loop control will be proposed to improve the accuracy of the voltage control scheme.

It should also be noted that the slopes of the VVCs depend on the system configuration. As discussed in D3.3, this shows that the capability of an inverter-based controllable device to adhere to a set-point is more linked to the system topology, system impedance, and the location that this inverter has been installed at.

The intercepts of the VVCs in each system configuration (outage of each inverter) are presented in **Table 3-3**. As can be seen, the intercepts not only depend on the system level defined objective (according to **D3.3**), but also highly depend on the system configuration (here, the availability of the system controllable devices).

As discussed in **D3.3**, the intercept *c*, should closely match the optimal voltage (V_{opt}), i.e., the voltage set-points extracted for voltage control mode of operation. This shows the efficiency of the proposed method for active voltage management based on VVCs and validates application of the optimal voltages (V_{opt}) as the voltage set-points of the system inverters in the voltage control mode of operation. Similar to **D3.3**, he relative error is defined as the relative difference between the intercept of each VVC and the regarding optimal voltage ($|c\text{-}V_{opt}|/V_{opt}$)

For these studies,

Table 3-3 Intercepts of the VVCs in each system configuration (c constants for VVCs)

Unavailable inverter	**$V2G_1$**	**$V2G_2$**	**$V2G_3$**	**$V2G_4$**	**$V2G_5$**	**$V2G_6$**	**$V2G_7$**	**$V2G_8$**	**$V2G_9$**
Base case	0.98545	0.98953	0.98191	0.98282	0.98103	0.98757	0.97680	0.98615	0.98353
1	-	0.98051	0.97803	0.98175	0.97254	0.97920	0.97564	0.97201	0.97280

2	0.98326	-	0.97943	0.98018	0.97278	0.97834	0.97536	0.97799	0.97300
3	0.98087	0.98369	-	0.97738	0.97046	0.97466	0.97453	0.97233	0.97978
4	0.98534	0.98059	0.97771	-	0.97357	0.97533	0.97521	0.97816	0.97247
5	0.98352	0.98167	0.98119	0.98277	-	0.97599	0.97488	0.97200	0.97234
6	0.98868	0.98009	0.97910	0.98003	0.97279	-	0.97685	0.97185	0.97243
7	0.98154	0.98032	0.97837	0.97785	0.97281	0.97563	-	0.97285	0.97261
8	0.98141	0.98354	0.97884	0.98064	0.97028	0.97455	0.97626	-	0.97815
9	0.98074	0.97958	0.97585	0.97677	0.97598	0.97378	0.97465	0.97300	-

Table 3-4 shows the relative errors between the intercepts of VVCs and the regarding optimal voltages in voltage mode of operation for different system configurations. It is noticeable that in no configuration these relative errors exceed 0.25%. Another indication of the successful implementation of the proposed active voltage management technique on this sample system in different configurations.

Table 3-4 Relative errors between the intercepts of VVCs and the regarding optimal voltages in voltage mode of operation ($100*|c-V_{opt}|/V_{opt}$) in percent

Unavailable inverter	**$V2G_1$**	**$V2G_2$**	**$V2G_3$**	**$V2G_4$**	**$V2G_5$**	**$V2G_6$**	**$V2G_7$**	**$V2G_8$**	**$V2G_9$**
Base case	0.16000	0.04500	0.02300	0.13200	0.25100	0.24500	0.07400	0.14300	0.21800
1	-	0.06937	0.03364	0.08141	0.09551	0.01136	0.09667	0.10167	0.02943
2	0.07477	-	0.05874	0.02050	0.08107	0.05305	0.08024	0.10338	0.01824
3	0.05943	0.03569	-	0.02750	0.10184	0.04852	0.08839	0.06895	0.00378
4	0.00397	0.09041	0.00631	-	0.09557	0.00037	0.03973	0.08617	0.06157
5	0.09248	0.07236	0.03196	0.00585	-	0.03936	0.18095	0.10272	0.07563
6	0.01520	0.04585	0.05452	0.04783	0.07136	-	0.02162	0.11778	0.06106
7	0.01289	0.04236	0.05447	0.03807	0.06969	0.03595	-	0.11834	0.06956
8	0.09468	0.07844	0.00062	0.01431	0.07564	0.18327	0.03304	-	0.10976
9	0.01199	0.00701	0.03645	0.02606	0.05221	0.04484	0.01821	0.10279	-

In D3.3, the voltage profiles are compared with and without applying the proposed control algorithm. The necessity of keeping the VVC parameters updated for each inverter needs to be

shown and the effectiveness of the adaptive voltage control framework should be validated. For this purpose, two new studies are conducted.

For both studies, the minute by minute active and reactive power demands at all load points and also the other required data are collected for one week and for each minute a three-phase unbalanced power flow has been conducted to find the three-phase voltages. The input data were presented in **D3.3** and are not repeated here for the sake of brevity.

For both studies the proposed AVM algorithm is implemented in a one week period to keep the reactive power dispatch up-to-date. During each day of the study week a certain inverter is assumed to be unavailable. In the first day the first V2G system is unavailable, in the second day the second V2G system is unavailable and so on. V2G 8 and 9 are always available.

First study: In the week-long time-series power flow, the V2G systems on this sample LV feeder are tasked with following their assigned VVCs found in **D3.3**. In other words, the VVCs are not updated according to the availability of the V2G systems.

Second study: In a week-long time-series power flow, the V2G systems on this sample LV feeder are tasked with following their assigned VVCs found in this subsection. It means during each day, the set of VVCs are updated according to the outage of the regarding V2G system.

Table 3-5 and **Table 3-6** show the system energy loss and voltage unbalance index for the first and second studies, respectively. Each study has been repeated for the objectives of minimisation of the voltage unbalance and loss minimisation with different assumptions for the limitations that should be considered for the reactive power support capability of the system inverters. The details of such assumptions and also the definitions of the voltage unbalance index and total energy loss are provided in **D3.3** and is not repeated here for the sake of brevity.

Table 3-5 Energy loss and voltage unbalance for the First Study

Objective function and constraints		Total Energy Loss (kWh)	Average Voltage Unbalance
Min. Voltage Unbalance		301.0221	0.014872
Min. V. Unbalance with accurate operational constraints		302.2134	**0.013912**
Min. Voltage Unbalance Available NC Recommendation, Lagging PF>0.92		296.7859	0.015067
Min. Power Loss [kW]		288.9155	0.016153
Min. Power Loss with accurate operational constraints		**287.8015**	0.015543
Min. Power Loss [kW] NC recommendation Lagging PF>0.92		290.8570	0.016221
Fixed Power Factor	0.95 Lag Power factor	297.1450	0.017371
	Unity Power factor	298.9494	0.017235
	0.95 Lead Power factor	301.1108	0.017186

Table 3-6 Energy loss and voltage unbalance for the Second Study

Objective function and constraints		Total Energy Loss (kWh)	Average Voltage Unbalance
Min. Voltage Unbalance		308.4233	0.012621
Min. V. Unbalance with accurate operational constraints		305.2320	**0.012180**
Min. Voltage Unbalance Available NC Recommendation, Lagging PF>0.92		298.7541	0.015032
Min. Power Loss [kW]		284.8322	0.016503
Min. Power Loss with accurate operational constraints		**283.0875**	0.015854
Min. Power Loss [kW] NC recommendation Lagging PF>0.92		289.4841	0.016723
Fixed Power Factor	0.95 Lag Power factor	297.1450	0.017371
	Unity Power factor	298.9494	0.017235
	0.95 Lead Power factor	301.1108	0.017186

As can be seen in **Table 3-5** and **Table 3-6**, with the objective of minimisation of the voltage unbalance the value of the optimal voltage unbalance index is reduced at least by 14% in the second study compared to the first study.

The value of the total energy loss is reduced at least by 1.66% in the second study comparing to the first study where the loss minimisation is chosen as the system level objective function.

4. Conclusion and Future Works

Based on the results extracted in chapter 42, the role of online Wideband Systems Identification (WSI) technique in Dynamic Voltage Stability Monitoring (DVSM) scenario is very important. For both stability analysis and design of virtual output impedance controller, the knowledge of the grid impedance is crucial. Furthermore, the developed WSI tool needs to be non-invasive in the sense that it can be integrated into the controller hardware of the inverter as a software component. A non-invasive online WSI tool is developed adhering to the above-mentioned requirements. Simulation results and *Hardware-in-the-Loop (HiL)* results show the effectiveness of the developed WSI tool. Through the method of WSI both non-parametric and parametric impedance of the grid can be obtained. The grid impedance can be effectively identified by keeping the perturbation level under 5% of the nominal value. System level incorporation of WSI and its coordination is covered in *D3.5*.

An improvement to the existing WSI tool would be to incorporate orthogonal PRBS generation to identify impedances simultaneously and furthermore extend the impedance identification methods to sequence domain to include unbalance effects. An accuracy and uncertainty analysis is required to extensively understand the robustness in impedance estimation of the developed WSI tool.

The case studies conducted chapter 3 show the effectiveness of the proposed adaptive AVM algorithm based on the results of impedance identification technique to approximate the system configuration in the local control system of each inverter-based control devices. These results show that by updating the VVCs according to the system configuration, the values of the objective functions will be significantly improved and therefore, the AVM method remains resilient against the network changes. The adaptive VVCs enable the decentral operation of inverter-based control devices for voltage control in an online setting while the system configuration is varying from time to time, satisfying the performance criteria of the distribution system operator.

For each inverter-based controllable device, an optimal voltage was found for each possible network configuration. According to D3.3, these optimal voltages can be considered as the target voltages for an adaptive voltage control scheme, when the controllable devices are being operated under voltage control mode.

The proposed AVM algorithm still needs to be improved and there is still some practical issues that should be addressed. Most of these issues will be tackled in the remaining tasks defined in the present project where it has been tried to propose effective solutions to mitigate the regarding issues.

After application of VVCs and finding the new setting of each inverter it is quite possible that more corrections are required according to the new set of PCC voltages. A supervised closed-loop control will be developed **D3.5** to achieve a near optimal reactive power dispatch between the system controllable devices. Considering the proliferation of the RES in LV distribution systems, there may be some opportunities to control the load point voltages more effectively using these high control capacity. In **D3.5**, it has been tried to develop an algorithm to consider different objectives in the proposed decentralised static voltage control simultaneously.

In work package 5, the data of various trial sites will be provided by ESBN. Accurate simulations will be conducted for differing RES technologies taking part in the Irish trial sites. The AVM technique will be used to determine VVCs for these sample networks and the results will be discussed in detail.

5. List of Figures

6. References

[1] A. Riccobono and A. Monti, “Noninvasive Online Parametric Identification of Three-Phase AC Power Impedances to Assess the Stability of Grid-Tied Power Electronic Inverters in LV Networks,” *IEEE J. Emerg. Sel. Top. Power Electron.*, vol. 6, no. 2, pp. 629–647.

[2] Z. Staroszczyk, “A method for real-time, wide-band identification of the source impedance in power systems,” *IEEE Trans. Instrum. Meas.*, vol. 54, no. 1, pp. 377–385.

[3] D. C. R. Stiegler, J. Meyer, P. Schegner, “Measurement of network harmonic impedance in presence of electronic equipment,” in *IEEE Int. Workshop Appl. Meas. Power Syst. (AMPS), Aachen Germany,* pp. 49–54.

[4] D. S. T. T. Do, M. Jordan, H. Langkowski, “Novel grid impedance measurement setups in electrical power systems,” in *IEEE Int. Workshop Appl. Meas. Power Syst. (AMPS), Aachen Germany,* pp. 1–6.

[5] W. W. Y He, H. S. hung Chung, C tak Lai, X Zhang, “Active cancellation of equivalent grid impedance for improving stability and injected power quality of grid connected converter under variable grid condition,” *IEEE Trans. Power Electron*, 2018.

[6] A. Barkley and E. Santi, “Online Monitoring of Network Impedances Using Digital Network Analyzer Techniques,” in *Applied Power Electronics Conference and Exposition, 2009. APEC 2009. Twenty-Fourth Annual IEEE, Washington, DC*, 2009.

[7] D. Martin, E. Santi, and A. Barkley, “‘Wide bandwidth system identification of AC system impedances by applying pertubations to an existing converter,’” in *Energy Conversion Congress and Exposition (ECCE), 2011 IEEE*, 2011.

[8] A. Riccobono, E. Liegmann, A. Monti, C. Dezza, and E. E. Santi, “‘Online wideband identification of three-phase AC power grid impedances using an existing grid-tied power electronic inverter,’” in *2016 IEEE 17th Workshop on Control and Modeling for Power Electronics*, 2016.

[9] B. Miao, R. Zane, and D. Maksimovic, “System Identification of Power Converters With Digital Control Through Cross-Correlation Methods,” *IEEE Trans.Power Electron*, vol. 20, no. 5, pp. 1093–1099, 2005.

[10] G. Francis, R. Burgos, D. Boroyevich, F. Wang, and K. Karimi, “An algorithm and implementation system for measuring impedance in the D-Q domain,” in *2011 IEEE Energy Conversion Congress and Exposition, Phoenix, AZ*, 2011, pp. 3221–3228.

[11] F. P. and A. M. A. Riccobono,E. Liegmann, M. Pau, “Online Parametric Identification of Power Impedances to Improve Stability and Accuracy of Power Hardware-in-the-Loop Simulations,” *IEEE Trans. Instrum. Meas.*, vol. 66, no. 9, pp. 2247–2257.

[12] E. S. Adam Barkley, “Improved Online Identification of a DC–DC Converter and Its Control Loop Gain Using Cross-Correlation Methods,” *IEEE Trans. Power Electron.*, vol. 24, no. 8, pp. 2021–2031.

[13] D. S. T. T. Do, M. Jordan, H. Langkowski, “Novel Grid Impedance Measurement Setups in Electrical Power Systems,” *Appl. Meas. Power Syst. (AMPS), 2016 IEEE Int. Work.*

[14] M. C. Sumner, M, Palethorpe, B, Thomas, D.W.P.; Zanchetta, P, Di Piazza, “A technique for power supply harmonic impedance estimation using a controlled voltage disturbance,” *IEEE Trans. Power Electron.*, vol. 17, no. 2, pp. 207–215.

[15] T. Roinila, T. Messo, and A. Aapro, “Impedance measurement of three phase systems in DQ-domain: Applying MIMO-identification techniques,” in *2016 IEEE Energy Conversion Congress and Exposition (ECCE), Milwaukee, WI*, 2016.

[16] K. McKenna and A. Keane, “Open and Closed-Loop Residential Load Models for Assessment of Conservation Voltage Reduction,” *IEEE Trans. Power Syst.*, vol. PP, no. 99, 2016.

[17] Q. Wang *et al.*, “Hybrid control strategy of grid-tied inverter for harmonic and reactive power compensation,” in *Proceedings of the 13th IEEE Conference on Industrial Electronics and Applications, ICIEA 2018*, 2018.

[18] P. Garcia, M. Sumner, A. Navarro-Rodriguez, J. M. Guerrero, and J. Garcia, “Observer-Based Pulsed Signal Injection for Grid Impedance Estimation in Three-Phase Systems,” *IEEE Trans. Ind. Electron.*, 2018.

[19] X. Wang, F. Blaabjerg, and W. Wu, “Modeling and analysis of harmonic stability in an AC power-electronics- based power system,” *IEEE Trans. Power Electron.*, 2014.

[20] P. Richardson, D. Flynn, and A. Keane, “Local Versus Centralized Charging Strategies for Electric Vehicles in Low Voltage Distribution Systems,” *Smart Grid, IEEE Transactions on*, vol. 3, no. 2. pp. 1020–1028, 2012.

[21] A. O’Connell, “Unbalanced distribution system voltage optimisation,” in *PES Innovative Smart Grid Technologies Conference Europe (ISGT-Europe), 2016 IEEE*, 2016, pp. 1–6.

[22] A. O’Connell, D. Flynn, and A. Keane, “Rolling Multi-Period Optimization to Control Electric Vehicle Charging in Distribution Networks,” *IEEE Trans. Power Syst.*, vol. 29, no. 1, pp. 340–348, Jan. 2014.

[23] M. Bakhtvar and A. Keane, “A study of operation strategy of small scale heat storage devices in residential distribution feeders,” in *PES Innovative Smart Grid Technologies Conference Europe (ISGT-Europe), 2017 IEEE*, 2017, pp. 1–6.

7. List of Abbreviations

AVM Active Voltage Management

B2B Business to Business

BMS Building management system

CAPEX CAPital EXpenditure

CENELEC European Committee for Electro technical Standardization

CEP Complex Event Processing

COTS Commercial off-the-shelf

CPMS Charge Point Management System

CSA Cloud Security Alliance

EMS Decentralised energy management system

ESS Energy Storage Systems

DER Distributed Energy Resources

DMS Distribution Management System

DMTF Distributed Management Taskforce

DSE Domain Specific Enabler

DSO Distribution System Operator

EAC Exploitation Activities Coordinator

ERP Enterprise Resource Planning

ESB Electricity Supply Board

ESCO Energy Service Companies

ESO European Standardisation Organisations

ETP European Technology Platform

ETSI European Telecommunications Standards Institute

GE Generic Enabler

GNC Generalised Nyquist Criterion

HEMS Home Energy Management System

HiL Hardware in the Loop

HV High Voltage

I2ND Interfaces to the Network and Devices

ICT Information and Communication Technology

IEC International Electro-technical Commission

IoT Internet of Things

KPI Key Performance Indicator

LV Low Voltage

M2M Machine to Machine

MPLS	Multiprotocol Label Switching
MV	Medium Voltage
NIST	National Institute of Standards and Technology
O&M	Operations and maintenance
OLTC	On-load tap changing
OPEX	OPerational Expenditure
OPF	Optimal Power Flow
PCC	Point of Common Coupling
PLL	Phase Lock Loop
PM	Project Manager
PMT	Project Management Team
POI	Points of Interest
PPP	Public Private Partnership
PWM	Pulse Width Modulation
PMU	Phasor Measurement Unit
PV	Photo Voltaic
QEG	Quality Evaluation Group
RES	Renewable Energy Source
S3C	Service Capacity; Capability; Connectivity
SCADA	Supervisory Control and Data Acquisition
SDH	Synchronous Digital Hierarchy
SDN	Software Defined Networks
SDOs	Standards Development Organisations
SET	Strategic Energy Technology
SET	Strategic Energy Technology
SG-CG	Smart Grid Coordination Group
SGSG	Smart Grid Stakeholders Group
SME	Small & Medium Enterprise
SoA	State of the Art
SON	Self Organizing Network
SRF	Synchronous Reference Frame
SS	Secondary Substation
SSAU	Secondary Substation Automation Unit
TL	Task Leader
TM	Technical Manager
TRL	Technology Readiness Level

V2G	Vehicle to Grid
VPP	Virtual Power Plant
VVC	Volt-var Curve
VVO	Volt-var Optimisation
WP	Work Package
WPL	Work Package Leader
ZIP	Z (impedance) , I (current) P (power) load model

Annex

A.1 VVCs of Available V2G Systems After the Outage of V2G Systems 2-4 and 6-9

For the sample system used to showcase the proposed adaptive AVM algorithm in this chapter (see subsection **3.4)**, the VVCs were presented in D3.3 assuming all the V2G systems are available. In subsection **3.4**, the sets of VVCs of the V2G systems were presented in the case of the outage of V2G systems 1 and 5. Other sets of VVCs are presented in **Figure 0-1**-**Figure 0-7**.

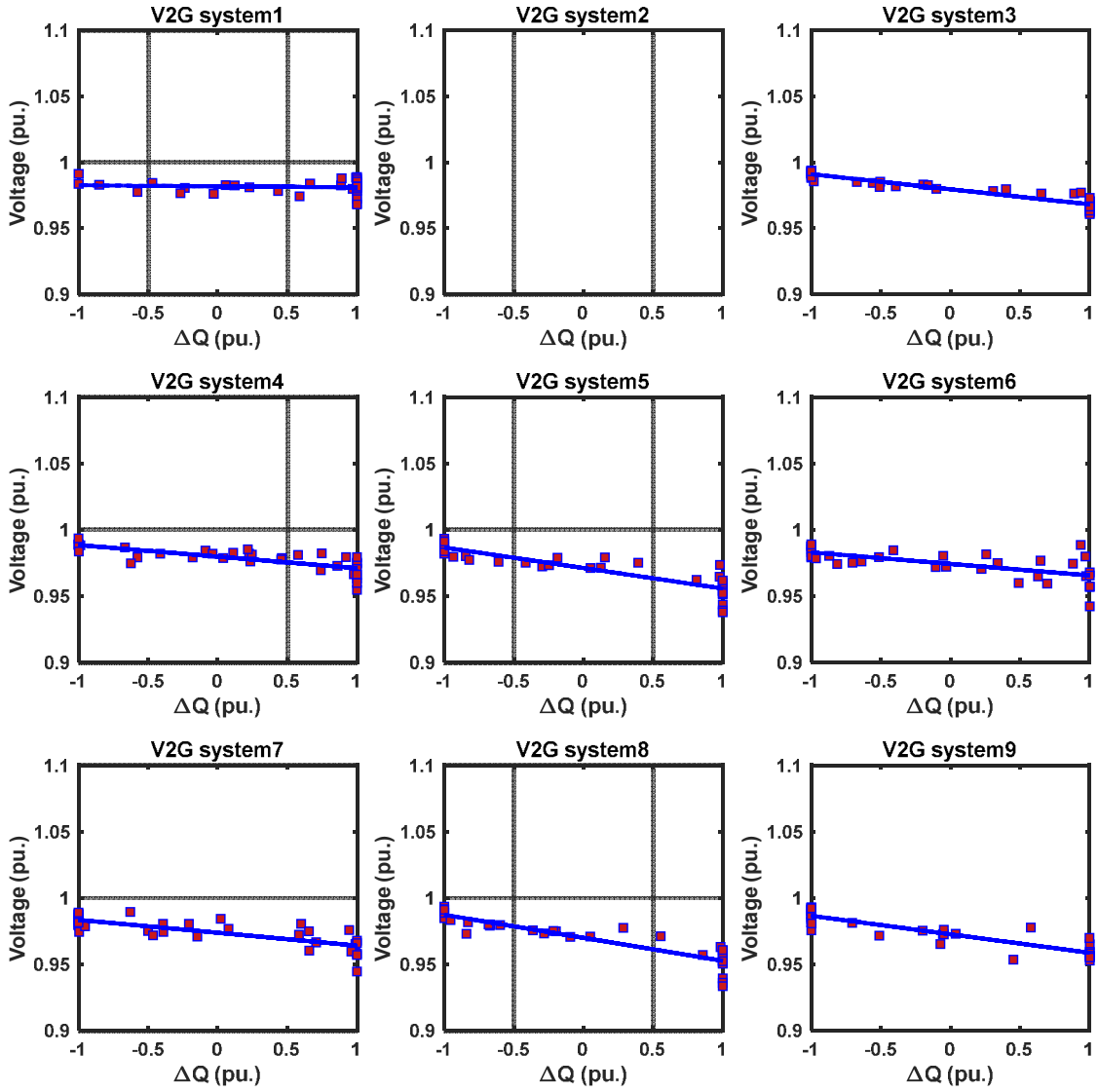

Figure 0-1 Resulting VVCs found for minimisation of voltage unbalance for V2G systems 1 and 3-9, showing intercepts and slopes assuming V2G system 2 is unavailable.

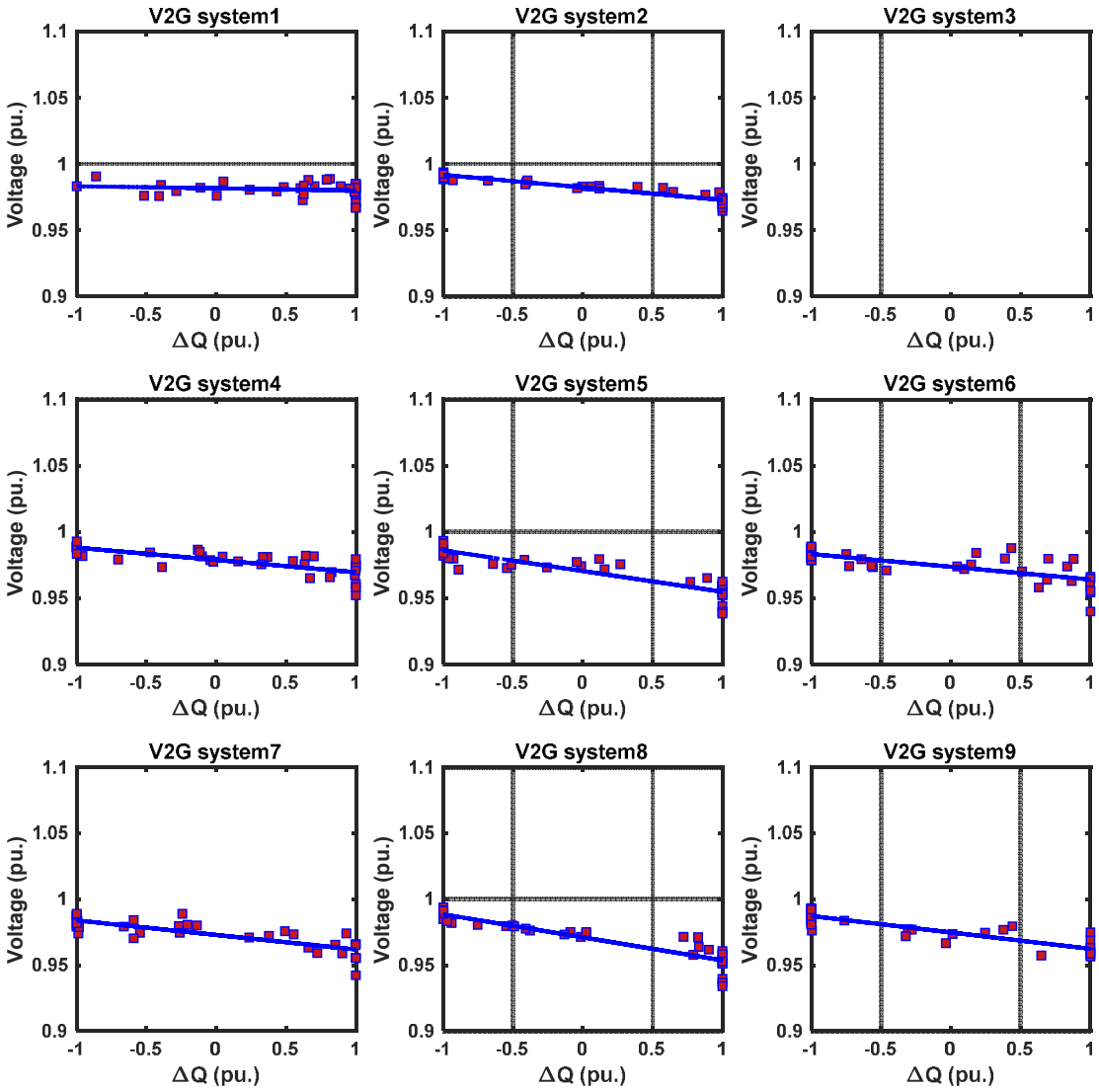

Figure 0-2 Resulting VVCs found for minimisation of voltage unbalance for V2G systems 1-2 and 4-9, showing intercepts and slopes assuming V2G system 3 is unavailable.

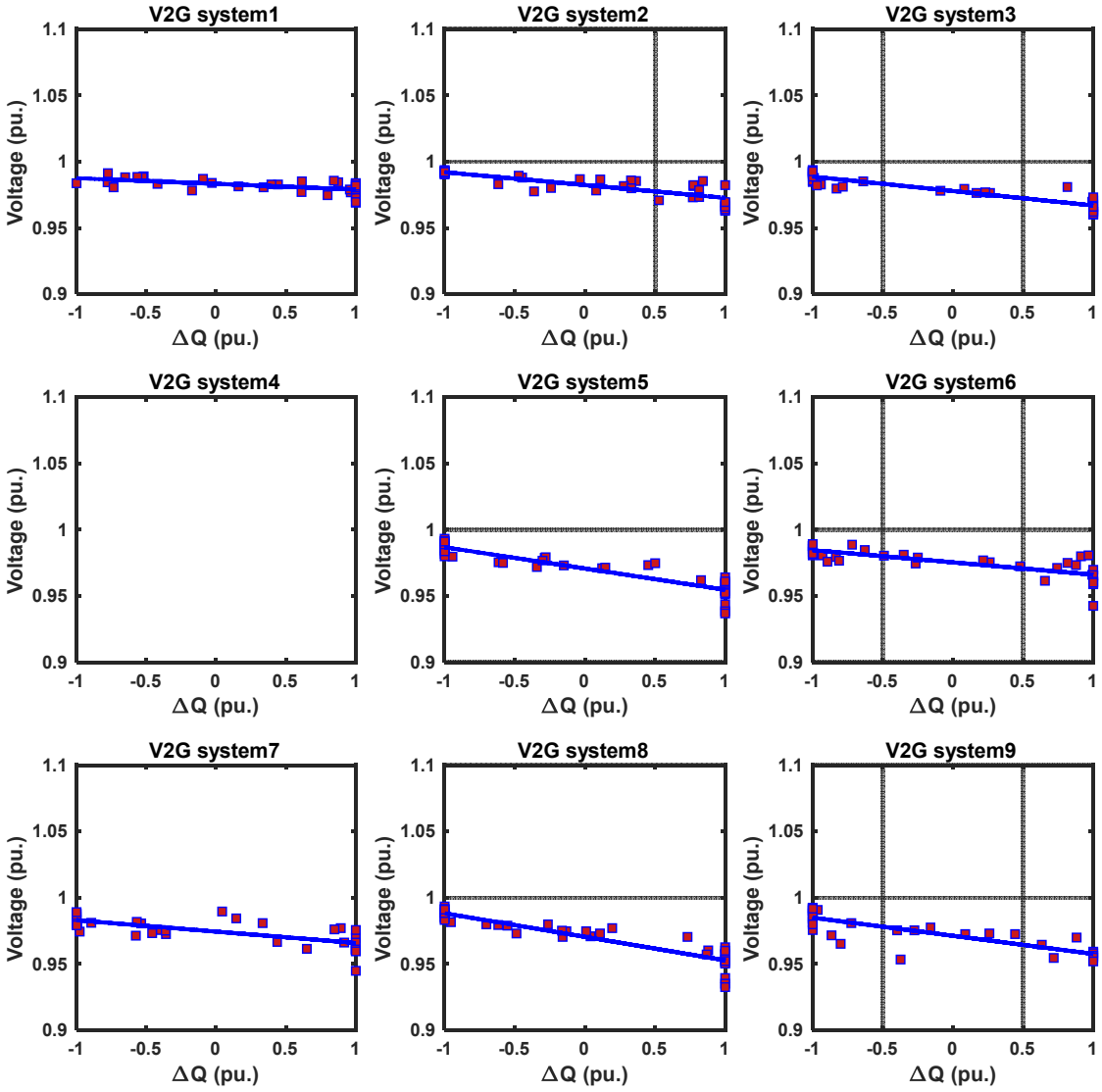

Figure 0-3 Resulting VVCs found for minimisation of voltage unbalance for V2G systems 1-3 and 5-9, showing intercepts and slopes assuming V2G system 4 is unavailable.

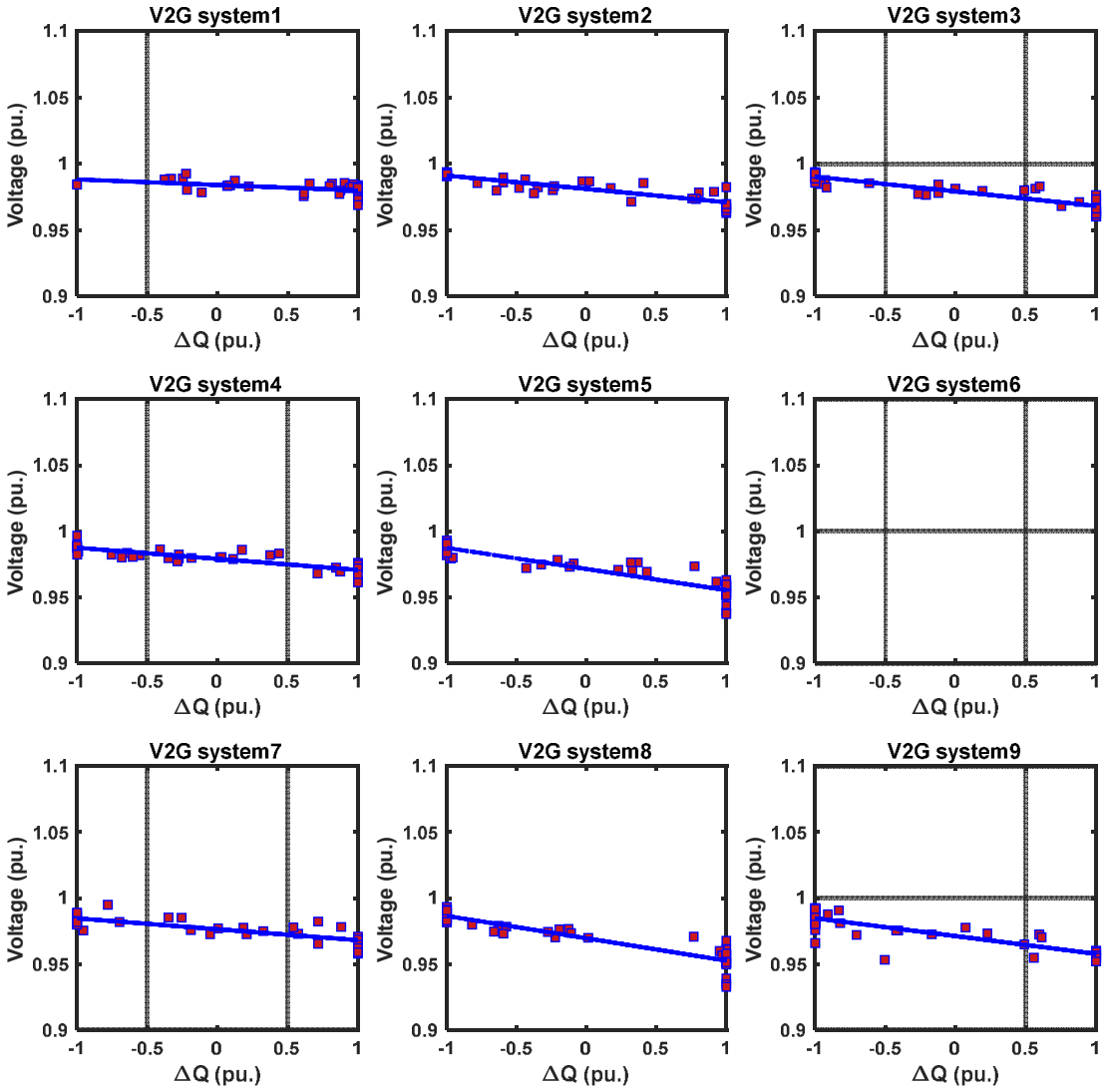

Figure 0-4 Resulting VVCs found for minimisation of voltage unbalance for V2G systems 1-5 and 7-9, showing intercepts and slopes assuming V2G system 6 is unavailable.

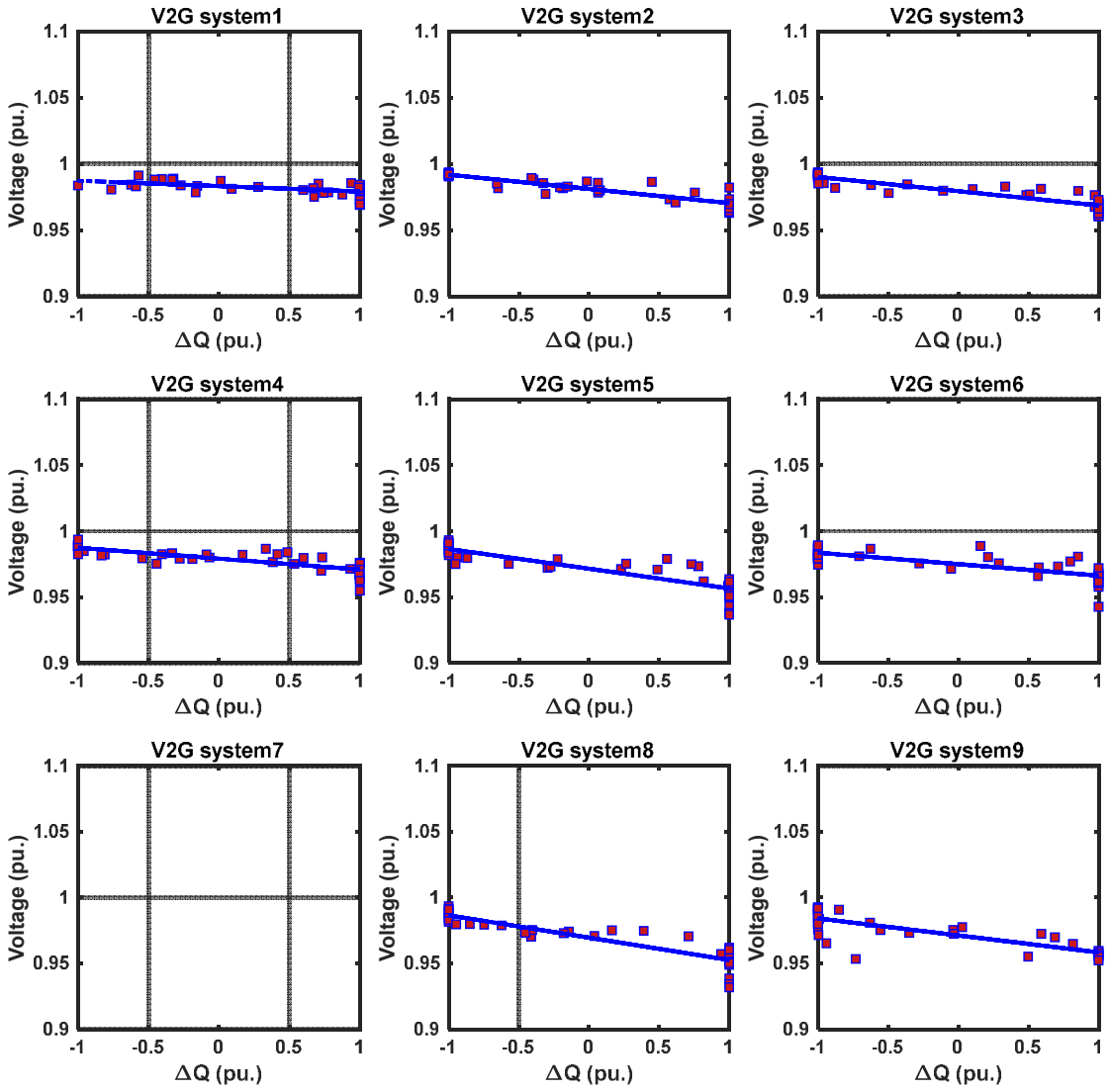

Figure 0-5 Resulting VVCs found for minimisation of voltage unbalance for V2G systems 1-6 and 8-9, showing intercepts and slopes assuming V2G system 7 is unavailable.

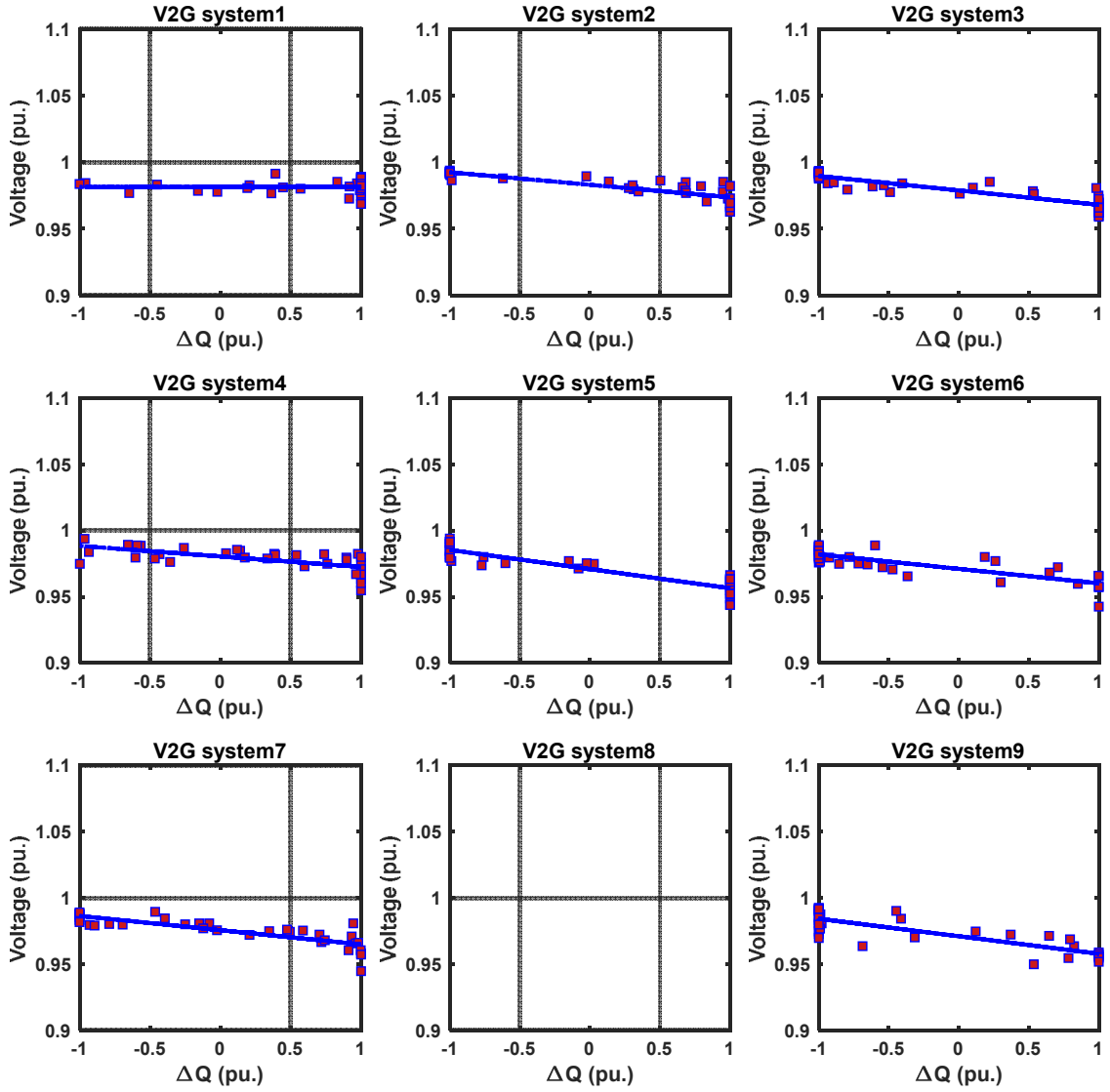

Figure 0-6 Resulting VVCs found for minimisation of voltage unbalance for V2G systems 1-7 and 9, showing intercepts and slopes assuming V2G system 8 is unavailable.

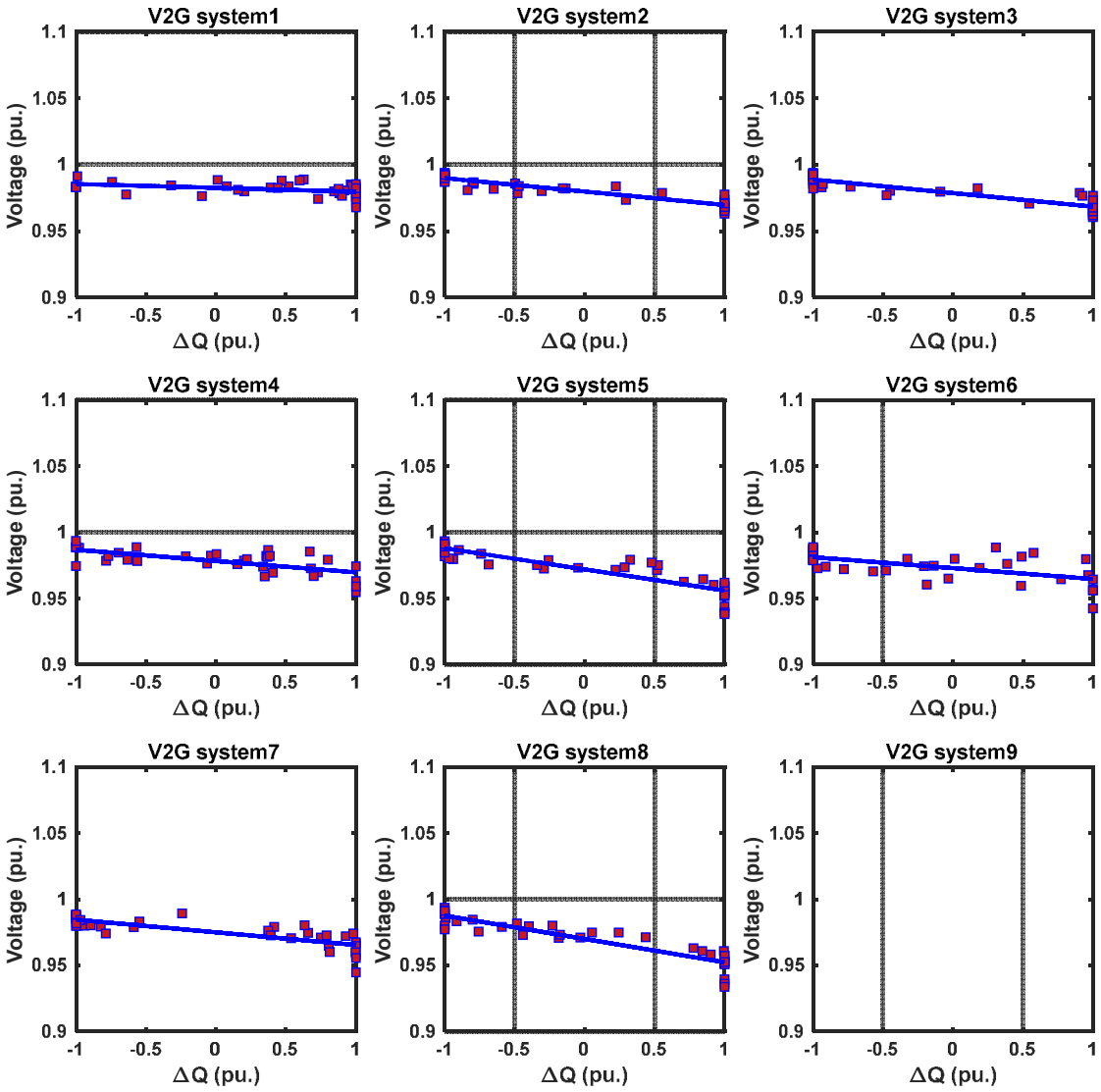

Figure 0-7 Resulting VVCs found for minimisation of voltage unbalance for V2G systems 1-8, showing intercepts and slopes assuming V2G system 9 is unavailable.